MASTER'S THESIS

How does the grid scale support accurate spatial memory and navigation?

TORGEIR WÅGA *Department of Neurosciecne, NTNU*

Supervisor
LISA M. GIOCOMO

Co-supervisor
MAY-BRITT MOSER

(PAGE UNINTENTIONALLY
LEFT BLANK.)

ACKNOWLEDGEMENTS

First and foremost I would like to acknowledge and thank Lisa M. Giocomo for her guidance and advice throughout the course of this thesis. She gave me the opportunity to explore areas of science I only dreamed of just a few years ago, and always provided guidance when I was lost.

I would also like to thank all the rest of the people at the Kavli Institute, for all the help and support I have gotten throughout my time here. A special thanks to David Rowland for providing us with transgenic mice and teaching me the methods. Also a special thanks to Kyrre Haugen who taught me all I know about how to do histology. And a special thank you to the animal technicians for taking care of all the wonderful animals. And thank you to the mice.

I also have to thank Maria for joining me in the insanity of the few last months of the project, making me feel somewhat normal despite the lamentable state I was in. And Eline for not judging me too harshly while observing my decline.

I tried.

Contents

SUPPLEMENTARY MATERIAL

How does the grid scale support accurate spatial memory and navigation?

TORGEIR WÅGA *Department of Neurosciecne, NTNU*

ABSTRACT

How does the grid scale support accurate spatial memory and navigation? This critical piece of the puzzle is currently missing from experimental work on grid cells. Previous research has demonstrated that the medial entorhinal cortex (MEC) is required for accurate spatial memory and navigation. But few studies have examined the importance of grid scale in these same processes. Here, we examine how the topographical organization of grid scale contributes to spatial memory and navigation by using behavioral paradigms combined with optogenetic manipulations. Multiple tasks were utilized; object exploration, the Barnes maze and a spatial delay non-match-to sample task in an 8-arm radial maze. We hypothesize that optogenetic photoinhibition of the smallest grid scale will reduce spatial accuracy, resulting in mice showing impairments when asked to discriminate between spatial locations at a fine spatial resolution. The results indicate that the dorsalmost MEC is crucial for spatial memory and navigation, and might be especially important for recognizing and relating to a novel spatial change in the environment. We also demonstrate behavioral experimental designs that may be used in further experimentation with optogenetics.

1. INTRODUCTION

The ability to encode, retrieve, and consolidate episodic memory - the memory for events of your everyday life – and the ability to successfully navigate through the environment, both rely on the same brain structures in the medial temporal lobe (**Figure 1**). In 1953, William Beecher Scoville, an American neurologist, carefully resected large portions of the medial temporal lobes from the brain of Henry Molaison (HM) with the intention of relieving him of his terrors of debilitating epileptic seizures. Unintentionally, Scoville also relieved HM of his memory (Scoville and Milner, 1957). The unfortunate consequences of a temporal lobectomy has since been shown to include both the ability to retrieve past episodic memories and the ability to store new episodic memories, and the level of impairment reflect the extent of the bilateral resection. In the case of HM, this included most of the intraventricular portion of the hippocampus, the amygdaloid complex, and the entire entorhinal cortex, leaving what little was left of the hippocampal formation void of cortical inputs (Corkin et al., 1997). The surgically induced anterograde amnesia observed in HM spurred a new interest in hippocampal research focused on its role in memory in monkeys and rodents. The initial efforts to reproduce the effects seen in HM were fruitless however(Douglas, 1967), mainly due to the lack of appreciation for the distributed learning and memory systems in the brain (Squire, 2004).

Figure 1 | Parahippocampal- hippocampal circuitry. Billions of single receptors are each activated by different specific changes in the environment around the organism. Each of the cells containing the receptors are activated upon some threshold of change, and fire an action potential. Electrochemical activity from groups of cells with similar but slightly different activation patterns is propagated to cells one synapse away, where the joint activity from the upstream cells are integrated and might exceed the threshold for further downstream propagation, and the process is repeated. Thus, there is an addition to the information content of each such interaction, where the receiving cells represent a more complex representation of the external space than the cells upstream. Activity from motor areas producing output patterns, and sensory feedback within the motor system, like proprioception, provides additional information in the converging activity in higher order processing stream. The activity propagation patterns of information processing are initially constrained to specific modalities, but eventually reach polymodal association areas. At the top of this hierarchy of information processing is the hippocampal/parahippocampal areas (Lavenex and Amaral, 2000).

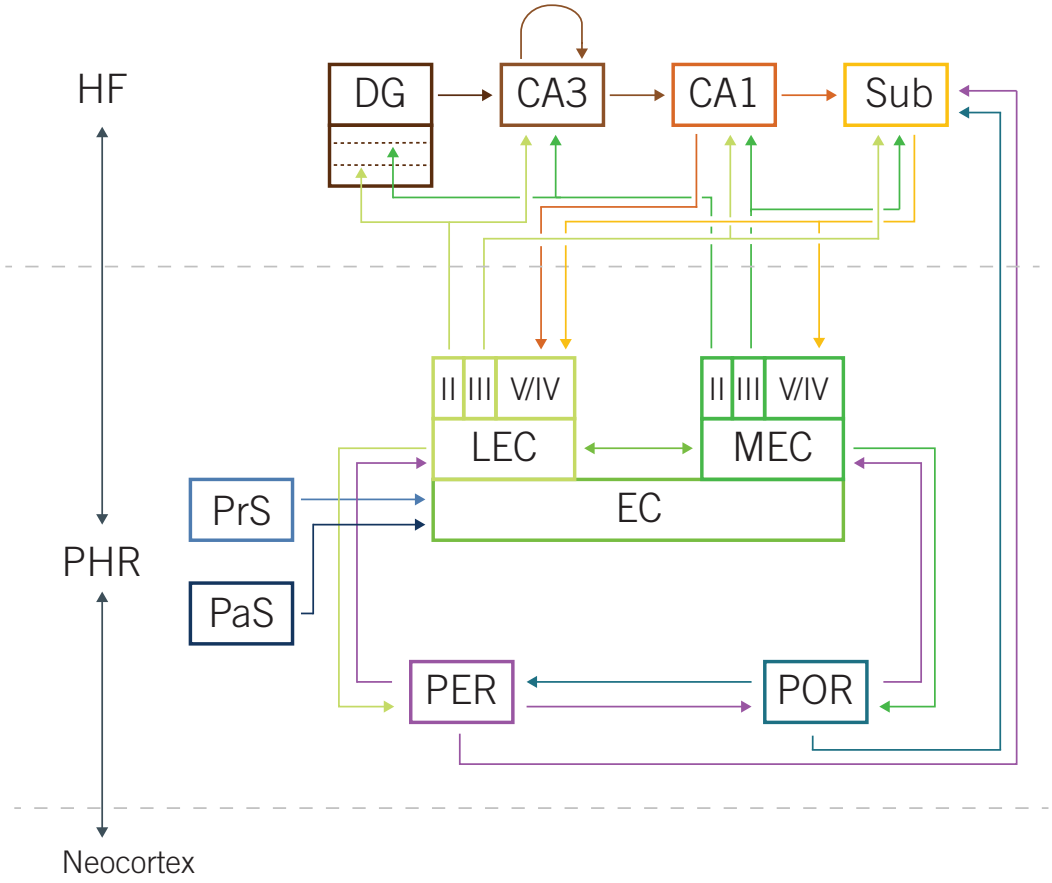

In rodents, the perirhinal (PER 35/36) and postrhinal (POR) cortices in the parahippocampal region (PHR) receive converging inputs from both unimodal and polymodal association areas, and propagate the activity to the entorhinal cortex. Preferentially neurons PER innervate cells in the lateral entorhinal cortex (LEC) while axons of POR neurons terminate in the medial entorhinal cortex (MEC). The axons of the MEC, and LEC layer II cells project to and terminate in the outermost two thirds of the dentate gyrus molecular layer (DGml) in the hippocampus, innervating the dendrites of the same granule cells with soma located in the granule cell layer (DGgcl). These projections, called the medial (from MEC) and lateral (from LEC) perforant pathway, terminate in the middle 1/3 and the outer 1/3 of the DGml, respectively. The DG granule cells project to the CA3 neurons which are massively recurrently connected, as well as sending collaterals to the CA1. Layer II neurons in MEC and LEC also project directly to the same calls in the CA3. Layer III neurons in MEC and LEC connect directly with cells located in distinct parts of the transverse axis of the CA1; the MEC targets cells located proximally within the CA1 and LEC target cells located distally within the region. And direct connections from these target regions go in the opposite direction, from CA1 targeting deeper layer cells in the entorhinal cortex at the same mediolateral area as the originating entorhinal cortex fibers. The same organization is seen between the entorhinal cortex of the subiculum (Sub), but with the proximodistal arrangement switched, with connections between the distal part of Sub and MEC and proximal parts of Sub and LEC. The CA1 region also connects to the MEC via the Sub, presubiculum (PrS), and parasubiculum (PaS) (Naber et al., 2001; van Strien et al., 2009; Witter, 2011).

Figure adapted from (van Strien et al., 2009).

1.1. HIPPOCAMPUS AND THE NEURAL CODING OF SPACE

The process of determining where we are in an environment, remembering that position and using the memory of that location to guide our behavior all depend on the presence of a neural representation of external space. The idea of an internal representation of space was first suggested by Tolman (Tolman, 1948). Tolman's ideas were based on experiments where rats were trained to retrieve a food reward from a specific location, with a long winding alley as the only possible route leading to the reward. When the rats were familiar with the route, the experimenters opened 18 previously unexplored straight alleys in a sunburst maze and blocked the alley to the winding path. The rats would reliably choose to run down the one new arm leading directly to the food reward (Tolman et al., 1946), indicating that the location of the reward was stored in the brain, similar to a marking on a map. And that this representation was stored separately from the representation of the winding path (Tolman, 1948). Summarizing the results of multiple behavioral studies on rats, Tolman proposed the idea of a 'cognitive map', an internal spatial map that supported an animal's ability to navigate in complex spatial environments. Tolman's cognitive maps theory was in stark contrast to the prevailing strict stimulus/response type of learning that dominated the theory of the field at the time. Instead, Tolman proposed that the environmental relationships between routes and places were stored as cognitive maps, which could be used to navigate to goals, rather than just re-playing out a stimulus-response sequence to a learned path/goal.

Such a specific internal representation of location necessitates a representation of distance and orientation, as well as a specific marking on the map representing the food reward. One such substrate is found in the hippocampus, where principal neurons fire selectively at high frequencies when the rat is moving through a specific portion of the environment. Called 'place cells', these neurons may represent markers of specific locations in such a cognitive map (O'Keefe and Dostrovsky, 1971). Soon after their initial discovery, it was found that different place cells fired at different specific regions in the environment, or place fields, and that place fields of relatively few cells could cover the entire environment, each cell represent-

ing a discrete region of the environment (O'Keefe, 1976). The same cell would show place fields in different environment, and the location of the place field would change across environments. Different place cells would switch place field in a seemingly unrelated manner, indicating the cells together maintain a unique representation of each encountered environment (O'Keefe and Conway, 1978). O'Keefe recognized they might have found something major – a measurable and replicable neural activity underlying a higher-order cognitive function – the neurobiological underpinnings of Tolman's cognitive maps (O'Keefe and Nadel, 1978).

Since O'Keefe first described them in the 1970's, place cells have been the focus of intense study. Research has revealed a great diversity in external factors that influence the activity patterns of the place cells and that there is a functional divide between the place cell populations of the CA1 and the CA3 area, as suggested by the difference in intrinsic connectivity of these two areas. The pyramidal cells of the CA3 are highly recurrently connected and receive input directly from layer II of the entorhinal cortex, as well as indirectly via the dentate gyrus. The pyramidal cells of the CA1, on the other hand, show no recurrent connections and receive cortical input directly from layer III of the entorhinal cortex as well as from the principal cells of CA3 (Amaral and Witter, 1989). These anatomical differences may support the emergence of different functional properties between the two CA regions of the hippocampus.

The properties of place cells are typically studied by chronically implanting electrodes in the hippocampus of rats or mice and recording the activity of cells while the rodent forages freely. Usually in strictly cue-controlled geometrical environments, like a square or circular enclosure. From early on, it was found that the measured place field of a cell would follow the rotation of a cue card in otherwise uniform environments (O'Keefe and Conway, 1978; Muller and Kubie, 1987), suggesting that place fields are anchored to visual cues in the local external environment. Subsequent studies have demonstrated that the place fields of a cell might also be modulated by auditory (Moita et al., 2003), olfactory (Save et al., 2000), or tactile (Gener et al., 2013) cues, suggesting the complete sensory experience of the animal is integrated in the place map.

In recording from the CA1/CA3 areas in a familiar environment, place fields of a subset of place cells will remain stable, with the longest stable place field recorded for 153 days (Thompson and Best, 1990; Lever et al., 2002; Ziv et al., 2013). However, moving the animal from the familiar environment to a novel one results in firing only in a subset of the same place cells, but the spatial phase relationship is not maintained between these active place cells (Muller and Kubie, 1987; Redish et al., 2001). Moving the animal back to the familiar environment results in the place cells reverting back to the firing patterns that were previously observed. Furthermore, in a familiar environment, the population of active place cells might change depending on behavioral demands. For example, in an experiment where rats had to avoid a rotating shock field only indicated by rotating cues and at the same time avoid a stationary shock field linked to stationary distal cues, activity in distinct populations of place cells were correlated with each shock field. Which population was active switched depending on which of the shock zones the animal was close to (Kelemen and Fenton, 2010). This tendency for the population activity of place cells to demonstrate a unique representation of each environment or encode particular information about the environment, is referred to as 'global remapping' (Colgin et al., 2008). This global remapping phenomenon may depend on recurrent connectivity in CA3. Such a recurrent network is ideal for completing a previously stored pattern through attractor dynamics (Marr, 1971). Thus, remapping is thought to reflect unique coding of different discrete environments. When an animal enters an environment, and it is sufficiently similar to a previous encounter, the activity pattern in CA3 cell populations will assume the activity pattern of the previous encounter. However, if the environment is dissimilar enough from previous encountered environments, the CA3 population will represent it with a new pattern (Lee et al., 2004; Leutgeb et al., 2004; Jezek et al., 2011; Mizuseki et al., 2012).

The seemingly random organization of place fields between different environments makes it possible for large numbers of neurons to encode spatial representations and support memory processes, while simultaneously making it easier to separate activity patterns between similar environments (Colgin et al., 2008). However, the unpredictable location of place

fields of single cells between different spatial environments suggests that the underlying representation of the spatial metrics of the environment must be calculated elsewhere (O'Keefe, 1976).

1.2. UPDATING THE HIPPOCAMPAL MAP - SPATIAL REPRESENTATION AND PATH INTEGRATION IN THE MEDIAL ENTORHINAL CORTEX

For many years, it remained unknown as to what types of spatial input place cells might be integrating. The feed-forward connectivity of CA1 certainly suggested that the place cell activity recorded there could originate elsewhere. Indeed, it was found that the place cell activity still persisted in the CA1 in rats after CA3 lesions (Brun et al., 2002), which left the direct entorhinal cortex afferents as the only extrahippocampal input. This discovery prompted a scientific expedition into the dorsolateral medial entorhinal cortex (MEC), which was known to project to the dorsal hippocampus, where place cells were usually recorded. This expedition led to the identification of several functionally defined cell types in the MEC, which embodied specific spatial features needed to maintain and continuously update the spatial metrics underlying the hippocampal place cell activity (Fyhn et al., 2004; Hafting et al., 2005; Sargolini et al., 2006).

One cell type that is abundant in the MEC is the head direction (HD) cell, which fires maximally when the nose of the animal is pointed towards a specific direction, regardless of their behavior or spatial location at the time. As a population of cells, all directions are represented (Taube et al., 1990a, 1990b) and so head direction cells function as a neural compass. Head direction cells were first recorded in the dorsal presubiculum (PrS, or postsubiculum) (Taube et al., 1990b), and later in the thalamus (Taube, 1995) ,the deep layers of the MEC (Sargolini et al., 2006), and the parasubiculum (PaS)(Boccara et al., 2010). The HD signal is thought to originate in subcortical circuits, an then propagated via the thalamus to the parahippocampal region where it provides directional tuning to the cell activity in the area (Clark and Taube, 2012).

Another cell type recorded in MEC, the border cell, represents the boundaries of the local environment (Solstad et al., 2008). Cells with similar properties have also been reported in the subiculum (Lever et al., 2009). Border cells selectively fire parallel to one of the borders in the environ-

ment, possibly playing a role in anchoring the directional signal to the environment (Solstad et al., 2008).

The last cell type identified in MEC, grid cells, might serve as a neural integrator of the distance traveled in the environment. Grid cells are particularly abundant in layer II of the MEC (Hafting et al., 2005), but also present in deeper layers of MEC, the PrS and PaS (Sargolini et al., 2006; Boccara et al., 2010). Like place cells, grid cells fire whenever the animal is moving through distinct fields in the environment. However, a single grid cell fires in multiple fields and creates a remarkable repeating triangular pattern that covers the entire floor of the environment. The grid pattern of neighboring cells have the same orientation, field size and spacing between fields, but the phase of the grid vertices are offset between cells (Hafting et al., 2005). Unlike the phases of the place cell fields, which remap unpredictably between cells in novel environments, the relative distance between the phases of two grid cells, as well as relative orientation and scale is fixed. As a consequence, as the animal moves through the environment, it will run through the fields of a sequence of cells with different phases, but with the directional relationship between any two cells always the same, such that the sequential firing of any series of active cells code the direction, speed, and distance the animal has moved. This stability of grid relationships across different environments strongly suggests that the grid cells form a metric representation of the environment that is largely independent of the situation or context (Fyhn et al., 2007).

Furthermore, the grid cells fire in the same loca-

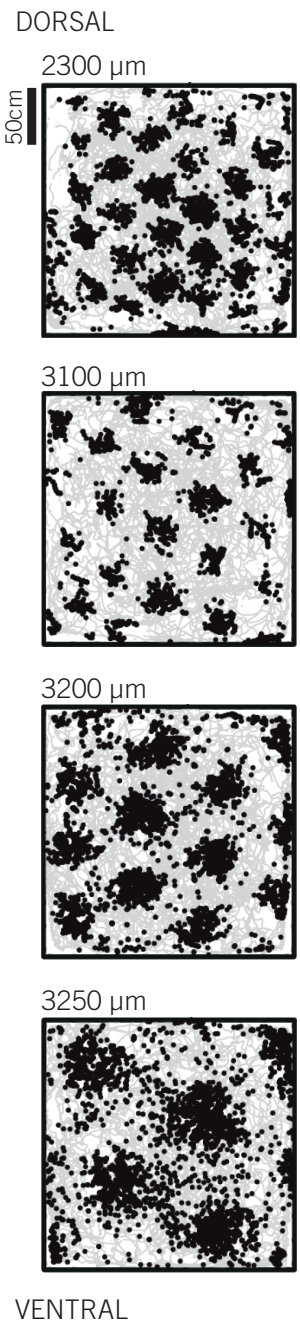

Figure 2 | Dorsoventral grid scale. Example grids at successive dorsoventral positions in a rat, with dorsoventral location from brain surface indicated in µm. Extracellularly measured action potentials (black) overlaid on the trajectory of the rat (grey). Reproducedwith permission from (Stensola et al., 2012)

tions, regardless of how fast the animal is moving, or which direction the animal is traveling. The maintenance of rigid grid periodicity in the dark (Hafting et al., 2005), suggests that grid cell activity is updated by idiothetic cues, and that grid cells are either functioning as path integrators or being updated by a path integration system (McNaughton et al., 2006). Indeed, in a study where rats were trained to rely on path integration to return a food pellet from an open field to a known safe refuge, sham operated rats returned directly to the refuge while entorhinal cortex lesioned rats went out in random directions searching for the safe refuge (Parron and Save, 2004).

1.3. THE GRID SCALE

Grids cells are interesting in that they are topologically organized along the dorsal-ventral axis of MEC according to spatial scale, with larger scales at increasing distances from the dorsal border of the MEC (Fyhn et al., 2004; Hafting et al., 2005; Brun et al., 2008). In previous recordings of grid cells, the dorsalmost recorded cells had grid spacing as small as 30 cm (Hafting et al., 2005; Fyhn et al., 2008) and largest spacing at 2.5-5 meters with 1.5-3 m wide fields (Brun et al., 2008). Grid scale does not increase continuously however, but rather in discrete steps, with partially overlapping modules occurring along the entire dorsal-ventral axis (**Figure 2**). The mean scale ratio between modules is close to 1.42, such that the hexagonal patterns of individual cells in each module covers double the area of the cells in the closest smaller scaled module (Stensola et al., 2012). Within each module, the spacing and size of the field, asymmetrical distortions, and the orientation of the grid is the same. Interestingly, the phase of the grids – the xy location of the grid vertices in relation to an external reference frame – is shifted (Hafting et al., 2005; Stensola et al., 2012), such that a very few grids may jointly represent specific locations in the entire environment. This phase shift across sets of grid cells allows the position of the animal to be reconstructed reliably from recorded data (Fyhn et al., 2007). Interestingly, the location preference of place fields in place cells may reflect input from grid cells with different spatial scales. If place cells receive input from overlapping grids of different scales, linear summation will lead to increased activity at specific locations compared to the rest of the environment (O'Keefe and Burgess, 2005; Fuhs and Touretzky, 2006; McNaughton et al., 2006;

Solstad et al., 2006). This theory is supported by the dorso-ventral increase in spatial scale of hippocampal place cells (O'Keefe and Burgess, 1996).

If an environment the animal is familiar with is extended or compressed, grid cells have been shown to rescale in the same direction as the environmental manipulation, and after repeated exposure to the manipulated environment, the grid regains its original arrangement (Barry et al., 2007). This rescaling appears to be module dependent; as the grid cells with the smallest grid scales rescale minimally, while grid cells with large scales may rescale completely. This module specific rescaling suggests that the grids of individual modules are differentially anchored to the external environment (Stensola et al., 2012). Grid cells also transiently rescale in novel environments (Barry et al., 2012). The MEC thus integrates idiothetic information with allothetic information and provide the hippocampus with structured spatially modulated activity.

1.4. THE HIPPOCAMPAL/ENTORHINAL SYSTEM IN MEMORY AND NAVIGATION

In parallel with the effort to document the spatially specific firing properties of the hippocampal/parahippocampal cells, behavioral studies have elucidated the specific role of these brain areas in memory and navigation. Due to the inherent difficulty of direct communication with rodents, their memory and navigation abilities are tested in experiments designed to take advantage of the species natural behavior, especially foraging food or avoiding potential dangers. Typically, brain structures of interest are ablated before learning, or neural activity in the area is temporarily disrupted during learning, to test the brain areas influence on acquisition. To test the brain areas influence on retention, the activity can be disrupted after the learning period.

An example of a commonly performed experimental protocol to test hippocampus-dependent memory is the water maze task. In the water maze task the animal is placed in a large circular pool of cold opaque water and learn to escape by finding and climbing onto a small platform hidden beneath the water surface (Morris, 1981; Morris et al., 1982). In subsequent trials, the animal is released from different locations in the pool and must utilize extramaze cues to locate the platform. The water is kept below the

body temperature of the animal, stressing it enough to quickly try to find land. Wild-type animals rapidly learn to swim directly for the hidden platform, suggesting they recall the previous location of the platform. Rats with complete hippocampal lesions do not learn the location of the platform in the water maze. They do improve slightly over trials, as measured in shorter escape latencies, but their swimming pattern shows no indication of knowledge of the location of the platform (Morris et al., 1982). The same disruption of spatial acquisition can be observed in animals with extensive entorhinal lesions (Schenk and Morris, 1985), lesions restricted to the medial entorhinal cortex (Steffenach et al., 2005), or by severing the perforant pathway, relieving the dentate gyrus of its entorhinal afferents (Skelton and McNamara, 1992). This suggests that the hippocampus and its entorhinal input are both necessary for acquiring spatial memories.

Conceptually, on the animals' first encounter with the task, the activity pattern of populations of hippocampal place cells is stored, presumably through plasticity between synapses in the dentate gyrus and CA3. Presumably, the entorhinal cortex interacts with the hippocampus to incorporate the relationships between the extramaze cues and the platform. Reintroducing the animal to the water maze, the familiar configuration of extramaze cues as perceived by the animal will result in similar activity patterns in the EC, encoding the metrics of the present observable environment, which again reproduce the hippocampal activity patterns, presumably by pattern completion in the DG/CA3, including the encoded location of the platform in CA1 (Dupret et al., 2010). Lesions in any of the relevant areas disrupt different steps of this process.

Van Cauter et al. (Van Cauter et al., 2013) performed a series of behavioral tasks in animals with complete extensive bilateral electrolytic lesion of the MEC. In the water maze task, MEC lesioned rats were impaired compared to sham operated and lateral entorhinal cortex (LEC) lesioned rats. Van Cauter et al. also performed a spatial and non-spatial recognition experiment where sham operated rats explored a displaced object significantly more than nondisplaced objects, while MEC or LEC lesioned rats did not show this preference. Van Cauter et al. supplemented these experiments with an experiment testing path integration ability of the rats in a

homing task in a cue stripped environment. On a circular platform with holes along the circumference, rats entered the platform through a specific hole and foraged for food in baited cups placed on the platform. The MEC lesioned rats showed a significantly lower number of direct returns to the start hole than the sham operated and LEC lesioned rats. The findings from these experiments support the hypothesis that spatial processing and path integration is dependent on the MEC, while non-spatial processing is dependent on the LEC.

While a functioning entorhinal cortex is necessary for accurate spatial memory and navigation, little is known about how the grid scale supports these processes. In this study, we examine how the topological organization of the grid scale contributes to spatial memory and navigation by using three behavioral paradigms combined with optogenetic inhibition. First, we performed two object exploration experiments to test the difference in the recognition of a spatial change and a non-spatial change. The object manipulations were done in both a small and a larger spatial extent. A Barnes maze experiment was done to test navigation and location memory. Finally, a spatial delayed non-match-to-sample protocol was done in the absence of spatial cues, and here we used either a large or a small difference between the start and goal arm in a radial maze. This last experiment was done to probe the functional role of the dorsal MEC in spatial memory and path integration.

Using transgenic mice with archeorhodopsin expression in the principal cells of layer II MEC, we transiently inhibit the activity of a subset of these cells in the dorsalmost MEC during experimental manipulation to probe the specific contribution of the principal cells in this area in the different behavioral paradigms.

We hypothesize that disrupting activity of a subset of the grid cells with the smallest grid scale will reduce spatial accuracy, resulting in an impairment when asked to discriminate between spatial locations at a fine spatial resolution.

2. GENERAL METHODS

1.5. THE MICE

Protocol testing was done with 20 male C57Bl/7 mice at X+- age, acquired from Charles River, Germany.

For the main experiments we used ENT x Arch transgenic mice (1 male, 11 female), acquired from David Rowland. This strain was originally generated in the lab of Cliff Kentros by crossing a tetracycline transactivator (tTa) line (Yasuda and Mayford, 2006) which used the promoter of the neuropsin gene to limit expression to the PrS, PaS and the outer layers of MEC, with an unpublished Arch line made in the Kentros lab, which utilize the outward proton pump ArchT (Han et al., 2011). The Arch expressed in our line is mainly restricted to layer II of MEC, and show expression of GFP in fibers and not cell bodies. Mayford noted the expected expression extent to be approximately 50% of layer II neurons of the MEC (Yasuda and Mayford, 2006). Previous histology of the strain suggest expression specifically in MEC layer II stellate cells, and electrophysiology suggest that only grid cells are affected by the photoinhibition which leads to total silencing of approximately 50 % of the grid cells recorded (unpublished data).

The transgenic mice were genotyped with two confirmed ENT x Arch+/+ before the experiment started, the rest of the mice had a 50% chance of being double positive. The mice were all implanted with optic fiber cannulas and went through testing in identical conditions. The ENT x Arch+/+ was confirmed by GFP expression in histology post mortem. During the testing the experimenter was blind to which mice were the sham operated control group, and which were in the experimental group.

All methods involving the use of live animals conformed to local regulations and the European Convention for the Protection of Vertebrate Animals used for Experimentation and Other Scientific Purposes. The well-being of all animals was checked daily by the experimenter, a veterinarian, or qualified animal caretakers.

The weight, whiskers, fur, barbing, and general health of each mouse were checked thoroughly before initiation and after the end of each experiment.

1.5.1.1. Housing and handling

1.5.1.0.1. Housing

The C57BL/6 animals were housed together with littermates in transparent cages with extensive enrichment. Some animals were moved to isolation in cages when fighting was observed.

Until surgery, the Ent x Arch animals were housed together with their littermates in transparent cages. After surgery, the mice were housed individually in transparent Plexiglas cages.

All mice were housed in a temperature and humidity controlled vivarium near the recording room and maintained on a 12 h light/ 12 h dark schedule, with ad libidum food and water. Testing occurred in the dark phase.

1.5.1.0.2. Handling

To minimize stress all mice were handled extensively before any testing began. All C57L/l6 housings included a red plastic 'tunnel'. At the start of each experiment the C57BL/6 walked into the 'tunnel' and the tunnel was lifted to the center of the testing environment where the mouse walked out (Hurst and West, 2010). The 'tunnels' were not used with the Ent x Arch mice, because of their implants and fibers connected. Instead, the Ent x Arch mice were handled extensively while the experimenter wore blue nitrile gloves until the mice walked freely onto the hand of the experimenter. This training was done by laying the hand stationary at the bottom of the cage of the unhandled mouse for 10-20 minutes with a few pieces of 'decorative cake sprinkles' (Dr. Oetker Mix) in the hand. The mouse would typically show an initial fear response and hide for a few minutes before a few sessions of approaching the hand followed by a brief body stretch and sniffing and running back to hide. After some such sessions the mouse would start investigating the hand and sleeve and at last climb up on the hand to eat sprinkles. The mouse was then briefly lifted and put down again, and the process was repeated. After repeating this procedure for 2-3 days, most mice climbed readily onto the experimenter's hand. At the beginning of experiments the Ent x Arch mice were picked up by holding a cupped hand close to the mouse and letting it walk onto the hand, and the mouse was

placed in the experimental area.

1.6. SURGERY AND IMPLANTS

Lisa M. Giocomo performed the surgery. Mice ranged from 6 months to 1 year of age at the time of surgery. On the day of surgery, the animals were first anesthetized with isoflurane (induction chamber level of 3.0% with an air flow at 1200 ml/min). This was gradually reduced once the animals were secured in the stereotaxic apparatus to 1% isoflurane with an air flow at 1000-1200 ml/min. In addition, an injection of buprenorphine was given immediately after the animal was secured in the stereotaxic apparatus (0.3 mg/ml). Levels of anesthesia were monitored by regularly checking the breathing rate as well as testing reflexes with toe and tail pinch. The mice were implanted bilaterally with a fiber cannula implant. The fiber was implanted at AP .4-.8 mm in front of the transverse sinus, 3.1-3.25 mm from the midline and 1.2 to 1.5 mm below the dura. The implants were angled 4-8 degrees in the posterior direction in the sagittal plane. The fiber was secured to the skull using small watchmaker's screws and dental cement. Following recovery of reflexes after anesthesia, the mice were returned to the housing room.

1.7. HISTOLOGY AND PHOTOMICROGRAPHY

1.7.1.1. Perfusion

After the last experiments were completed the animals were deeply anesthetized with isoflurane, and euthanized with a lethal dose of sodium pentobarbital (50mg/kg). The injection was followed by transcardial perfusion; first with 0.9 % NaCl solution then 4 % formalin. The whole brains were removed from the scull and stored in 4 % formalin solution for approximately one week before slicing.

1.7.2.2. Tissue sectioning

Before slicing, the cerebellum was cut off and the brain was parted in the midline with a scalpel. One hemisphere at a time was glued (Cryo glue tissue embedding medium, SLEE medical; or Richard-Allen scientific NEG 50, Thermo scientific) to an object holder and quickly frozen to approximately – 55 °C in the cryostat (SLEE Cryostat MEV) to avoid crystal for-

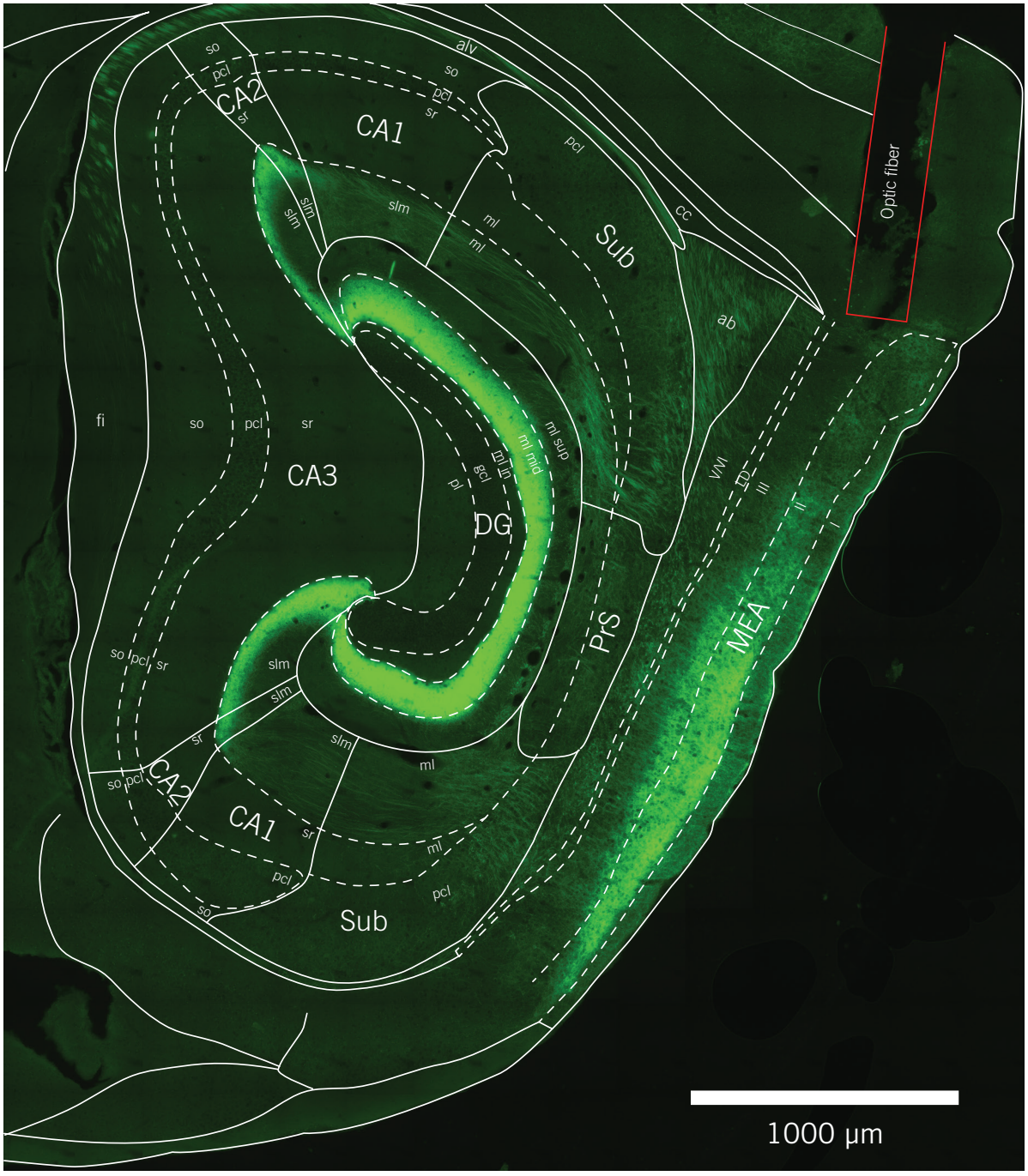

Figure 2 | Annotated sagittal 30µm slice from mouse 2205 right hemisphere (~ 3mm lateral from midline), showing the optic fiber implant position which left a lesion area outlined in red. Relevant structures are delineated in solid white lines, with substructure layers delineated with dotted lines. We can observe the expression of GFP which originates mainly in medial entorhinal area (MEA) layer II as can be verified from the dense termination in the dentate gyrus (DG) middle molecular layer (ml mid), as well as the deep part of stratum lacunosum moleculare (slm) of CA2 and CA3 (van Groen, Miettinen, Kadish, & Groen, 2003; Witter, 2007) [The de-

mation using the "quick freeze" function, while simultaneously spraying very lightly with cooling fluid (PRF 101 Cold spray) for ~10 seconds, and left in the "quick freeze" area of the cryostat for 8 minutes. Thereafter the object holder/brain was moved to the microtome of the cryostat and fixed to the holder where it was left for 30 min to defrost to proper cutting temperature. The chamber and object of the cryostat was kept at a constant temperature of -20 °C. Polisine slides (Thermo scientific) were coated with gelatin and left in an autoclave until it reached 100 °C, and then air-dried in ~23 °C for > 24 hours before use. Sectioning was done in 30 µm sagittal slices which were mounted directly to the slides from the microtome stage.

1.7.3.3. Staining

The brain slices were air-dried in ~23 °C for at least 24 h before staining. Every other slice was cleared with scale solution (1 µl triton X100, 500µl 8M urea, 200 µl 50% glycerol, 300 µl H2O) (Hama et al., 2011) to better define GFP expressing areas. The solution was dripped onto the slide with mounted slices, left for 10 min in -20 °C and cover slipped with SlowFade Gold Antifade Reagent (Invitrogen).

The remaining slices were stained with Cresyl Violet (Sigma). The slices were left 2 min in dH20, and then dehydrated by dipping the slides 10 times in 70-, 80-, 90, 100-, 100- and 100 % ethanol and leaving them 2 min in Xylene. They were rehydrated by dipping the slides 10 times in 100-, 100-, 100-, 90-, 80- and 70 % ethanol then left 5 min acetic acid. The slices were then washed quickly in cold running water, and left in Cresyl Violet solution for 6 minutes on a shaker in darkness. Surplus color washed away in cold running water, then alternately shaken quickly in acetic acid and left in running cold water until desired contrast is achieved. The slices were then dehydrated again and left for clearing in Xylene for > 5 min, before being cover slipped with Eukitt.

lineations were done on the basis of paxinos mouse brain atlas, allen mouse brain atlas, and what I learned from Witters seminars. They are approximate as they are done only from looking at the structures in this GFP slice (at 40x magnification) and the corresponding adjacent nissl stained slice. GFP can also be observed in the alveus (especially dorsal), maybe from MEA layer III neurons projecting to the CA1 via the temporoammonic pathway].

1.7.4.4. Microscopy and photomicrography

The sections were viewed using Carl Zeiss Axio microscopes, with a filter for GFP expression. Photomicrography was done with AxioVision and Neurolucida software, and delineation done in Adobe Illustrator CS6. An annotated version of a GFP expressing slice can be seen in **Figure 3**. Implant tracks for all the mice are available in the supplementary section at the end of the thesis.

1.8. OPTOGENETIC LIGHT DELIVERY

The laser used was a 532 nm, 200 mW, continuous wave DPSS laser (Shanghai Laser & Optics Century Co., Ltd. GL532T3-200) with beam diameter of 2.0+-0.2 mm and beam divergence, full angle: 1.5 +- 0.2 mrad.

The beam was reflected and guided by a visible broadband dielectric mirror (Thorlabs BB1-E02), through a continuously variable neutral density filter (Thorlabs NDC-50C-2M) and into a collimator (Thorlabs F220FC-B) to couple the free-space laser beam into an optical fiber. The other end of the optical fiber was coupled with an intensity divider (Doric mini cube intensity division) with output coupling to two 4 m fibers (Doric MFP_105/125/900-0.22_4m-SMA.2.5(F)) hung from pulleys in the roof into the experimental area so the mice could move freely while connected.

The angles of the mirror and the collimator were fine-tuned to achieve a Gaussian beam profile and similar intensity output in both fiber tips. The light intensity of each fiber tip was measured with a power meter (Thorlabs PM100D, with S120C photodiode power sensor) while modified to specified values by manipulation of the neutral density filter.

To minimize tissue damage, the fiber cannula implants had a relatively small 105 µm core, 125µm cladding, which restricted the numerical aperture (NA) to 0.22. The fibers used in the laser setup had the same properties to minimize loss at the connections between the parts of the laser setup.

S120c sensor measurement uncertainty = +-3%. (with beam diameter > 1mm)

The light transmission properties of the combined fiber and wavelength were calculated with the Brain tissue light transmission calculator provided by the Deisseroth lab (http://www.stanford.edu/group/dlab/) which predicts irradiance values based on earlier direct measurements in mammalian

brain tissue. The implant cannulas were tested for transmission properties post mortem, but most of the cannulas broke during the process of removing the brain from the cranium (Suplementary Table 1.).

To choose optic fibers appropriate for use in the experiments we went through several rounds of testing. The first fibers and connectors were made by the experimenter, but the diameter of 1 mm tubing proved too stiff and impeded the movement of mice. A second round made with thinner cladding worked fine with larger male mice (>40 g) but small females (<30 g) could not move freely. In the end we used .9mm tubing fibers provided by Doric, some with custom made connectors made by the experimenter and some with connectors preassembled provided from Doric. All fibers were tested thoroughly before use.

3. OBJECT EXPLORATION EXPERIMENTS

Object exploration tasks require the encoding of a complex spatial representation. We compared the exploration of objects during habituation and after a spatial or non-spatial change. In the spatial change sessions, the object was moved either a small (23 cm) or large distance (30 cm), to test small versus large spatial coding. In the non-spatial change, we replaced one object, retaining the same spatial configuration.

1.9. METHODS

1.9.1.1. Apparatus

The test environment was an open field box (50 x 50 cm wide, 50 cm tall) made of plastic, with exchangeable white plastic sheets wrapped over the floor and walls. The box was surrounded by dark blue ceiling-to-floor curtains. A camera (Bosch LTC0355) in the ceiling was centered above the maze and a single incandescent bulb (40 w) was placed next to the camera. A system of weighted pulleys in the ceiling made sure that the optic fibers could move effortlessly in all spatial dimensions at the level of the maze.

Two objects were placed in the open field at positions determined by the current task condition (**Figure 4**). To prevent a preference bias towards any of the objects, eight C57BL/6 mice (wild-type) were used in preliminary experiments that tested exploration activity on 12 different objects in

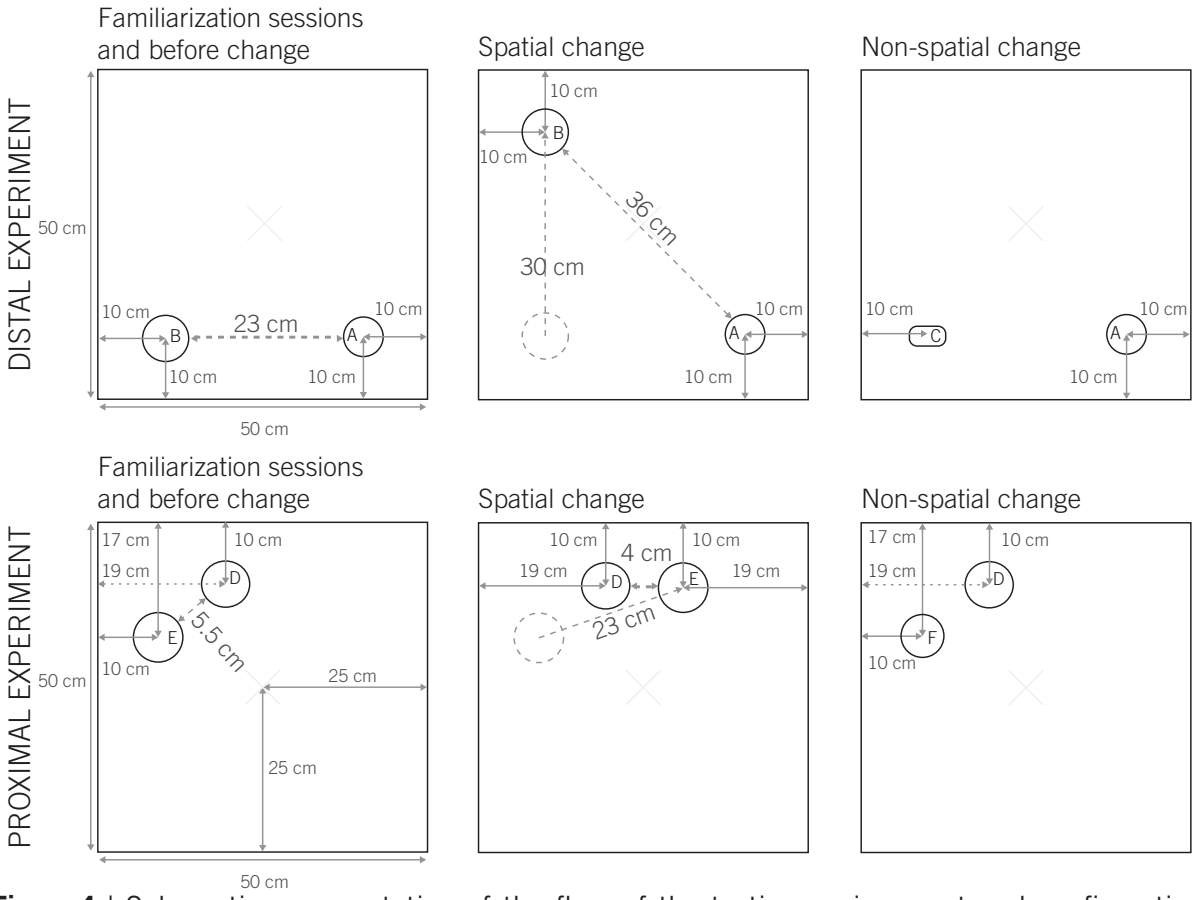

Figure 4 | Schematic representation of the floor of the testing environment and configuration of objects in different task conditions. The positions may vary within ± 0.5 cm between trials.

different combinations. The object combinations with similar exploration times in the object preference bias testing were later used in the protocol testing and in the main experiment. The objects used in the distal experiment were (a) a green glass container with a yellow and red plastic hat (16 cm tall, 6 cm ø), (b) a blue drinking glass with a red plastic hat (18 cm tall, 7 cm ø), and (C) a stack of pink plastic pop slice molds (17 cm tall, 5.5 cm × 3 cm wide). The objects used in the proximal protocol were (d) a conical colorless glass vase (18.5 cm tall, 7.3 cm ø), (e) a purple extendable play tunnel (18 cm tall, 7.5 cm ø), and (f) a colorless plastic bottle with a red cap (23 cm tall, 6.5 cm ø) (**Figure 5**). All of the objects were made of nonabsorbent materials that could be cleaned with alcohol without affecting the finish. When placed in the box, the objects were secured to the floor with removable adhesive tack (Faber-Castell, tack-it).

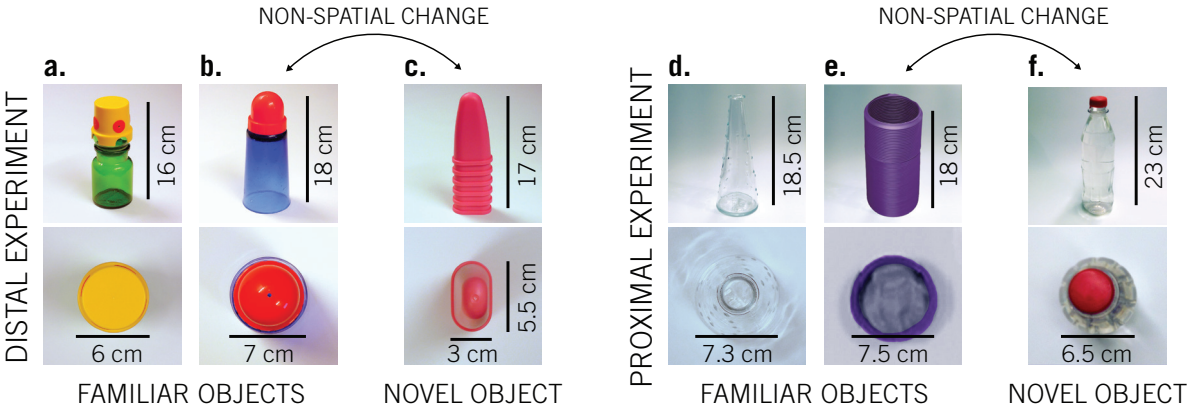

Figure 5 | Objects used in the exploration task. In the distal protocol, the objects used were a green glass container with a yellow and red plastic hat (a), a blue drinking glass with a red plastic hat (b), and a pink plastic pop sickle making containers stacked (c) replacing object 'b' in the nonspatial change. For the proximal protocol, the objects used were a conical glass vase (d), a purple extendable play tunnel (e), and a plastic bottle with a red cap (f) replacing object 'e' in the nonspatial change task. (All objects were acquired at IKEA, except for the plastic tunnel which is available at trixie.de)

1.9.2.2. Behavioral procedure

Prior to the experiments the mice were individually allowed to explore the empty open field freely for 10 minutes each day on two successive days. This was done to acclimatize the animals to the testing environment, allowing the mice to overcome neophobia, and allowing the experimenter to observe the mice for any deviations in health or behavior.

Both experiments - distal and proximal - as well as the protocol testing followed the same general procedure, with the location and type of objects as the only difference. The exception being that the protocol testing was done with unconnected wild-type mice. Each experiment lasted one week, excluding habituation.

First, the mice were submitted to 5 minute familiarization sessions, once a day for 5 days. In these familiarization sessions two objects were placed at fixed locations, and remained there for all sessions (**Figure 6 a**). The repeated exposure let the mice become familiar with the objects and their location and established the typical behavior which could be compared to the ensuing spatial and non-spatial test conditions.

Next followed the testing conditions; the mice were submitted to a spatial change test on day 6, and a non-spatial change test on day 7 (**Figure 6 b,c**). At the beginning of every session the mouse was placed in the middle

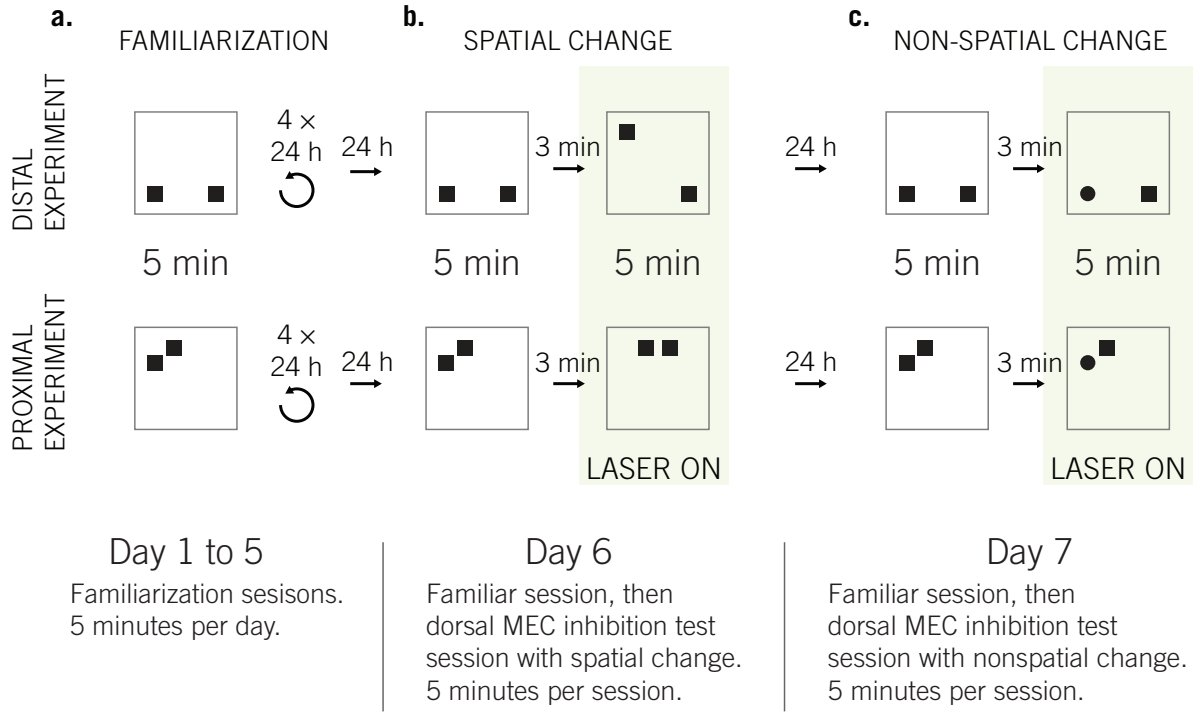

Figure 6 | Session layout for the exploration task. The only difference between the distal and proximal protocol was the location and type of objects (locations represented by black squares and circles). a) Familiarization. The objects were placed in the same configuration, and the mouse explored for 5 minutes per day for 5 days without inhibition. b) Spatial change. 5 minutes of exploration of objects in familiar configuration without inhibition. 3±1 minute between sessions interval, and then 5 minutes exploration with inhibition after one object is moved. c) Non-spatial change. 5 minutes of exploration of objects in familiar setting without inhibition. 3±1 minute between sessions interval, and then 5 minutes of exploration with inhibition after one object is replaced by a novel object.

of the field. On the testing days, the mice were first allowed to explore the familiar objects in familiar locations for 5 minutes followed by a 3 minute interval and a new 5 minute test session with manipulated objects. In the main experiments the laser was turned on to inhibit the dorsal MEC of the experimental group throughout the 5 minute test session. In the distal spatial change condition object 'b' was moved 30 cm relative to the room, and the distance between object 'b' and object 'a' increased from 23 cm to 43 cm. In the proximal spatial change condition object 'e' was moved 23 cm relative to the room, but kept the approximate 5 cm distance from the stationary object. In the distal non-spatial change condition object 'b' was replaced by object 'c', and in the proximal experiment object 'e' was replaced by object 'f' (**Figure 5**).

The walls and floor of the test environment were cleaned with 70 % ethanol and the objects were replaced by clean identical objects before every session and during the between session intervals of both test conditions.

1.9.3.3. Data analysis

All sessions were videotaped and stored for later analysis. To analyze the behavior we used Ethovision XT 8.5 software to track the nose-point and head direction of the mice throughout the 5 minute trials. The exploration time for an object was defined as the total amount of time the nose-point of the mouse was located within a defined zone of 2 cm distance from the edge of the objects with the nose-point directed towards the object (**Figure 7**). The videos with tracked paths were reviewed and the time the mice spent in the zones without exploring the object (sniffing, neck stretching) was removed from the data.

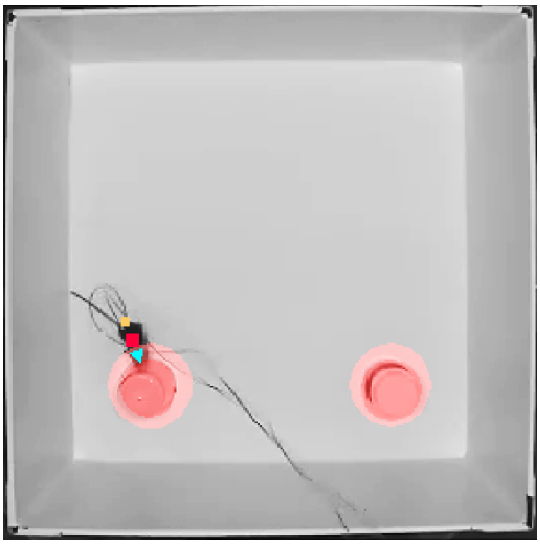

Figure 7 | Exploration zones in the object recognition experiment. Exploration was defined as whenever the nose-point of the mouse (blue triangle) was located within a zone of 2 cm distance from edge of the object (red zone)

Exploration times St and Mt, the combined total duration of time spent exploring the stationary or manipulated object, respectively, were used as within session variables. A discrimination ratio (DR) was calculated as (Mt – St) / (Mt + St), the time difference divided by the total exploration time. The resulting value is the relative proportion of time spent exploring the objects compared to the total amount of time spent exploring. The DR value will be -1 if the mouse only explored the stationary object, and +1 if the mouse only explored the manipulated object, while an equal amount of time spent exploring both objects results in a DR value of 0 (used by e.g. Langston & Wood, 2010).

To test the difference in exploration based on the observed behavior rather than of an optimal situation, one-sample two-tailed t-tests of the DR's were performed with the null hypothesis that the DR's were sam-

pled from a normal distribution with the observed mean (DRoμ). The DR observed mean was calculated as the DR averaged over all sections and all mice; if the mice show no object preference throughout the experiment the DRoμ will be 0.

In addition, to comparing exploration of the same object between sessions, we performed a paired-sample two-tailed t-test on the same object from session to session for both the stationary and the manipulated object, e.g. a comparison of how much object 'a' was explored in the session before to how much object 'a' was explored in the session after object 'b' was moved (Van Cauter et al., 2008). We did this in both test conditions.

1.10. RESULTS

1.10.1.1. Protocol testing

Initial object preference bias and testing indicated a difference in climbable and un-climbable objects. The mice would climb on top of the tallest climbable object and stay there for portions of the task. The shortest objects we tested (< 2 cm tall) were mostly ignored. This led us to choose objects which, from the object preference testing, we deemed tall enough to be un-climbable. Our judgment about climbability was not flawless. In the testing of the distal protocol originally 19 mice were tested, but 4 mice were excluded from the analysis for climbing object 'a' and staying on top of it. Still, a slight preference for object 'a' could be observed in most sessions.

Using a group of wild-type mice, we first demonstrate that they can detect novel objects after spatial and non-spatial changes. All results are reported in [mean±sem ,unit (seconds,sec; discrimination ratio,DR) test]. The discrimination ratio was significantly higher than the observed mean (-0.0056 DR) for both spatial [0.188±0.077 DR (mean±sem), one-sample $t(14) = 2.5$, $P < 0.05$] and non-spatial [0.283±0.094 DR, $t(14) = 3.1$, $P < 0.01$] changes in the distal configuration (**Figure 8 a**) but only for the non-spatial change [0.416±0.052 DR, $t(19) = 8.3$, $P < 0.001$] in the proximal condition (**Figure 8 b**). The proximal spatial condition proved very difficult for the mice to detect and further analyses focused on the distal condition. Future work could test different spatial configurations or distances to determine at

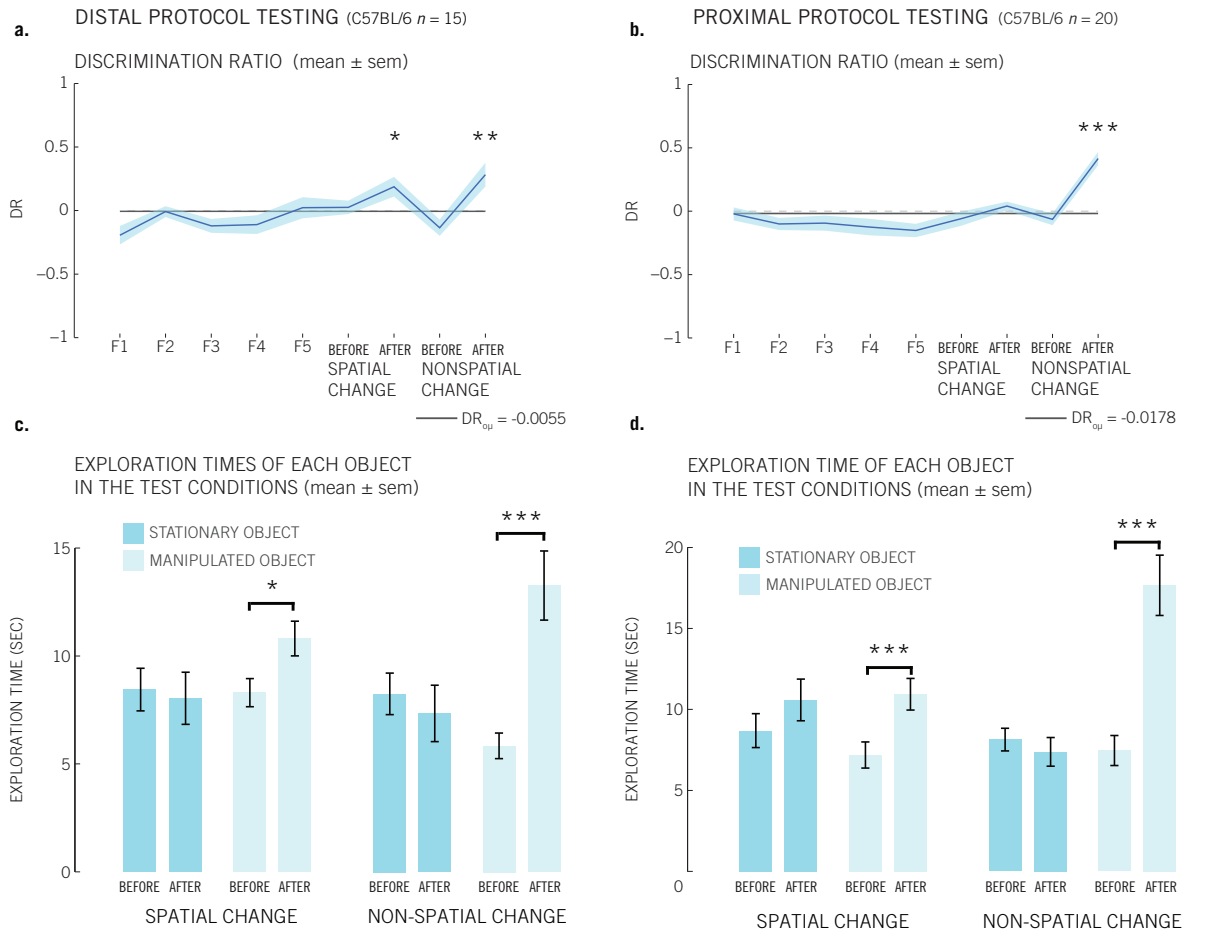

Figure 8 | Protocol testing for the object recognition experiment. Observed mean (DRoμ) = -0.0056 in the distal protocol, and -0.0178 in the proximal protocol. Discrimination ratio for the protocol testing of the distal experiment (a) and the protocol testing for the proximal experiment (b) shown with asterisks denoting significance in two-tailed t-tests against a mean of (DRoμ). Only directions towards the manipulated object are reported. c. and d. show the exploration times for each object compared to itself across trials. For the distal protocol testing (c) and proximal protocol testing, (d) paired sample t-tests were done for each object (*, $p < 0.05$; **, $p < 0.01$; *** $p < 0.001$).

what point the mice are able to detect a spatial change.

Tests were also done for changes in exploration of the same object between the two sessions of the same test condition. In the distal configuration, the wild-type mice explored the manipulated objects (moved object: [10.82±0.80 sec from 8.30±0.65 sec, paired sample $t(14) = 2.2$, $P < 0.05$], replaced object: [13.26±1.6 sec from 5.86±0.59 sec, $t(14) = 5.2$, $P < 0.001$]) significantly more after the change. The exploration time for the stationary objects did not differ significantly, with either the spatial or the non-spatial manipulation from the previous trial in the spatial condition [8.05±1.21 sec from 8.45±0.99 sec, $t(14) = -0.3$, $P = 0.75$] or the non-spatial condition

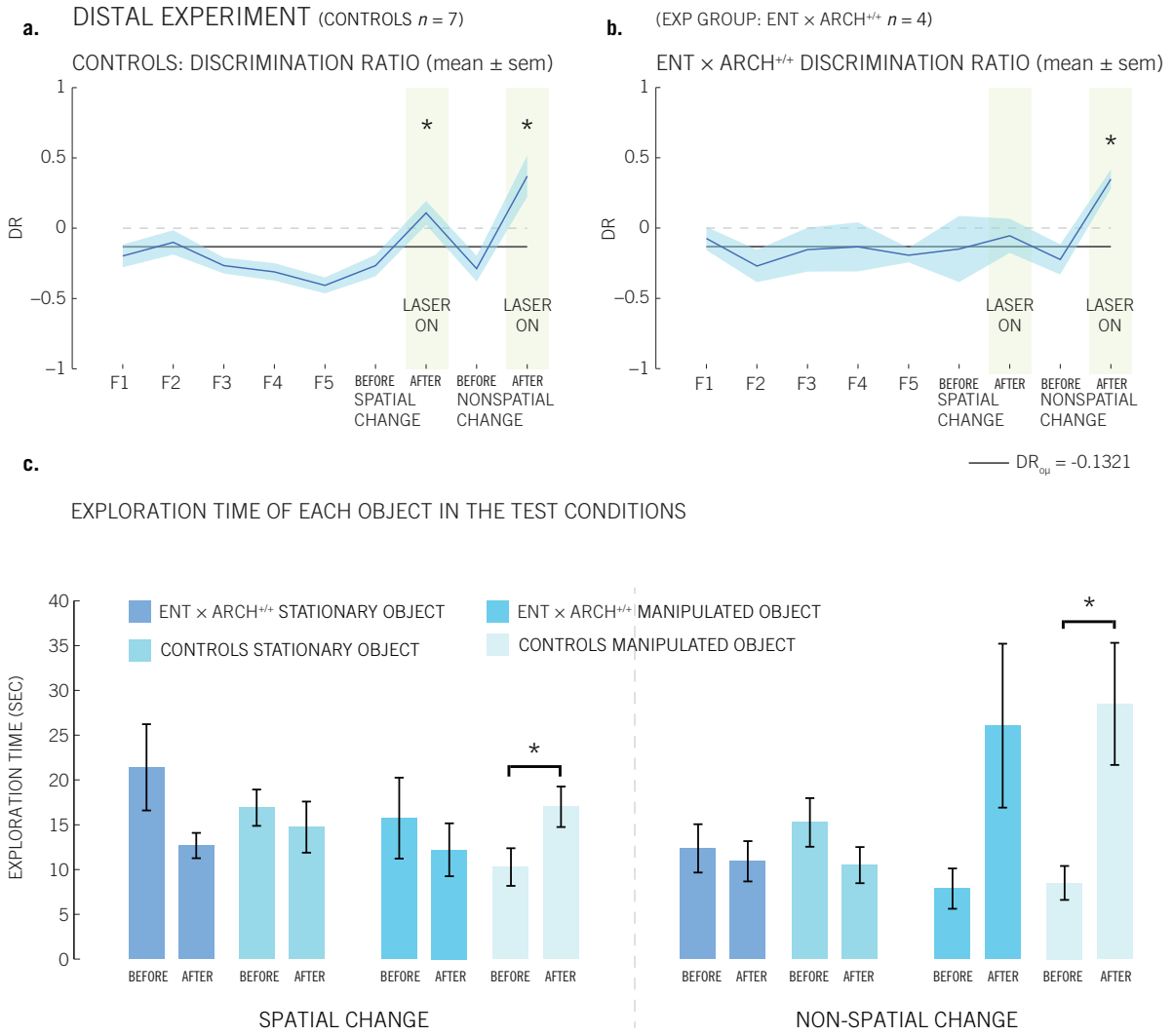

Figure 9 | Results for the distal object exploration experiment. Observed mean (DRoμ) = -0.1321. a) Discrimination ratio for the control group in the distal experiment. b) Discrimination ratio for the experimental group in the distal experiment. Asterisks denoting significance in two-tailed t-tests against DRoμ. Only directions towards the manipulated object reported. c) shows the exploration times for each object compared to itself across trials. Paired sample t-tests were done for each object (*, p < 0.05; **, p < 0.01; *** p < 0.001).

[7.34±1.31 sec from 8.26±0.96 sec, t(14) = -0.6, P = 0.55] (**Figure 8 c**)

The same was true for the proximal condition where the wild-type mice explored the moved object more after the move [10.94±0.98 sec from 7.18±0.81 sec, t(19) = 5.1, P < 0.001] and the replaced object more after the change [17.67±1.87 sec from 7.46±0.93 sec, t(19) = 5.4, P < 0.001] while the exploration time for the stationary object did not differ significantly in either condition (spatial change: [10.588±1.284 sec from 8.692±1.044 sec, t(19) = 1.5, P = 0.16], non-spatial change: [7.380±0.887 sec from

8.136±0.698 sec, t(19) = -0.7, P = 0.49]) (**Figure 8 d**).

1.10.2.2. Experiment

During laser stimulation, the discrimination ratio of the control group significantly increased compared to the preceding familiarization trial. In the distal configuration this effect was significant for both spatial [0.109±0.085 DR from -0.266±0.077 DR, paired-sample t(6)= 2.9, P < 0.05] and non-spatial changes [0.370±0.146 DR from -0.289±0.02 DR, t(6) = 3.3, P < 0.05]. In the experimental group, the discrimination ratio was not significantly different from the preceding familiarization trial for the spatial change condition [-0.054±0.122 DR from -0.148±0.235 DR, t(3) = 0.4, p = 0.72] but was significantly different for the non-spatial change condition [0.349±0.069 DR from -0.223±0.107 DR, t(3) = 3.3, P < 0.05].

In the distal experiment, for the control group, the discrimination ratio was significantly higher than the observed mean (-0.1321 DRoμ) in both the spatial change [0.370±0.146 DR, one-sample t(6) = 3.4 P < 0.05] and the non-spatial change [0.109±0.085 DR, t(6) = 2.8, P < 0.05]. For the experimental group the discrimination ratio was significantly higher than the observed mean in the non-spatial change [0.349±0.069 DR, t(3) = 7.0, P < 0.01] but not the spatial change condition [-0.054±0.122 DR, t(3) = 0.6, P = 0.57] (**Figure 9 a, b**).

We also looked at the change in exploration of each object after the object manipulation compared to before. In the control group the change in exploration was significant for the manipulated, but not the unchanged objects (moved object: [17±2.26 sec from 10.27±2.26 sec, t(6) = 2.9, P < 0.05], replaced object: [28.5±6.82 sec from 8.47±1.9 sec, t(6) = 2.5, P < 0.05] , unmoved object: [14.73±2.86 sec from 16.9±2.09 sec, t(6)=-0.8 P = 0.47], nonreplaced object: [10.49±2.02 sec from 15.26±2.72 sec, t(6)= -1.4, P = 0.21]). In the experimental group, no significant change in exploration was seen for any of the objects. However, all mice explored the changed object more than the unchanged, while the opposite was true for the moved object.

For the proximal experiment, the discrimination ratio was significantly higher than the observed mean (-0.0268 DRoμ) for the non-spatial change for both groups (controls: [0.465±0.101 DR, t(5) = 4.9, P < 0.01], exper-

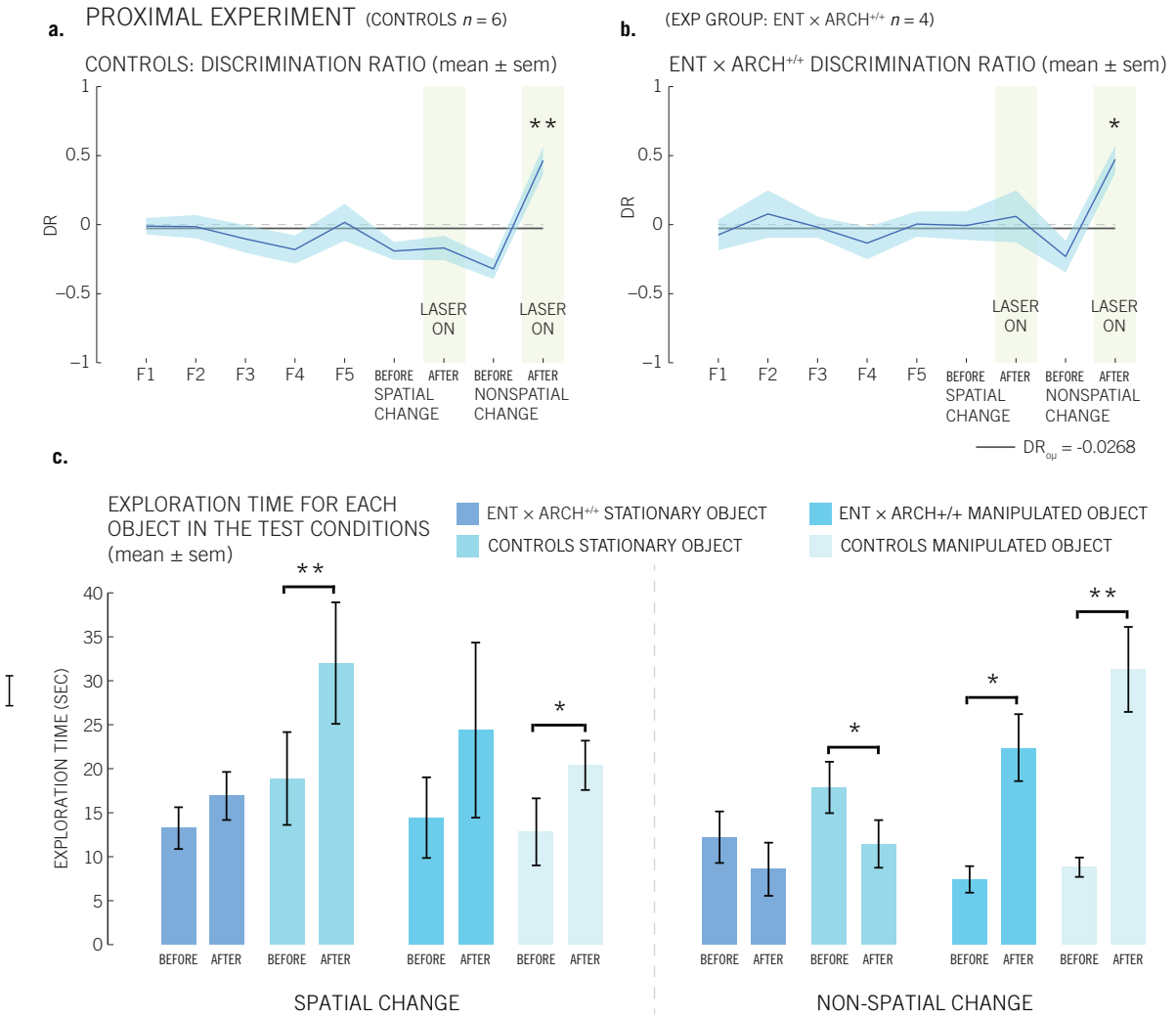

Figure 10 | Results for the proximal object exploration experiment. a) Discrimination ratio for the control group in the proximal experiment. b) Discrimination ratio for the experimental group in the proximal experiment. Asterisks denoting significance in two-tailed t-tests against a mean of (DRoμ). Only directions towards the manipulated object reported. c) Shows the exploration times for each object compared to itself across trials. Paired sample t-tests were done for each object (*, $p < 0.05$; **, $p < 0.01$; *** $p < 0.001$).

imental group: [0.474±0.1 DR, $t(3) = 5.2$, $P < 0.05$]). This effect was not seen for the spatial change experiment (controls: [-0.169±0.089 DR, $t(5) = -1.6$, $P = 0.17$], experimental group: [0.06±0.188 DR, $t(3)=0.5$, $P = 0.68$]) (**Figure 10 a,b**).

However, after object manipulation, the control group had a significantly higher exploration time of the both manipulated objects (moved object: [20.33±2.8 sec from 12.68±3.82 sec, $t(5)=3.6$, $P > 0.05$], replaced object: [31.23±4.83 sec from 8.74±1.1 sec, $t(5) =4.6$, $P < 0.01$]), as well

as the unmoved object [31.95±6.9 sec from 18.83±5.28 sec, t(5) = 4.3, P < 0.01]. The experimental group, on the other hand, had significantly higher exploration time only for the replaced object (replaced object: [22.36±38 sec from 7.45±1.5 sec, t(3) = 3.9 , P < 0.05], moved object [24.42±9.96 sec from 14.46±4.589, t(3) = 1.6 , P = 0.20], nonreplaced object:[8.61±3.02 sec from 12.24±2.93 sec, t(3) = -1.1 , P = 0.37], unmoved object: [17±2.73 sec from 13.28±2.38 sec, t(3) = 0.9, P = 0.45]) (**Figure 10 c**).

4. BARNES MAZE EXPERIMENT

The Barnes maze is a circular, open arena with multiple holes located around the circumference of the environment. The bright nature of the arena motivates the animal to find the location of a single escape box. The experiment is designed to test spatial learning and memory.

1.11. METHODS

1.11.1.1. Apparatus

For this task we constructed a Barnes maze – an elevated polycarbonate circular platform (Lexan, 90 cm ø, 1 cm thick) with 16 holes placed with equal distance along the circumference such that each hole is separated by a 22.5 degrees angle originating from the center of the maze (**Figure 11**). The circular platform was covered with a white exchangeable plastic sheet. In order to facilitate the removal of the escape box while mice were still connected to the optic fibers, 4 mm wide slits were cut from the holes to the outer edge off the disk. All holes except for the escape hole were closed from below the maze with a piece of removable dull black plastic, leaving a 1 cm from the floor of the maze to the

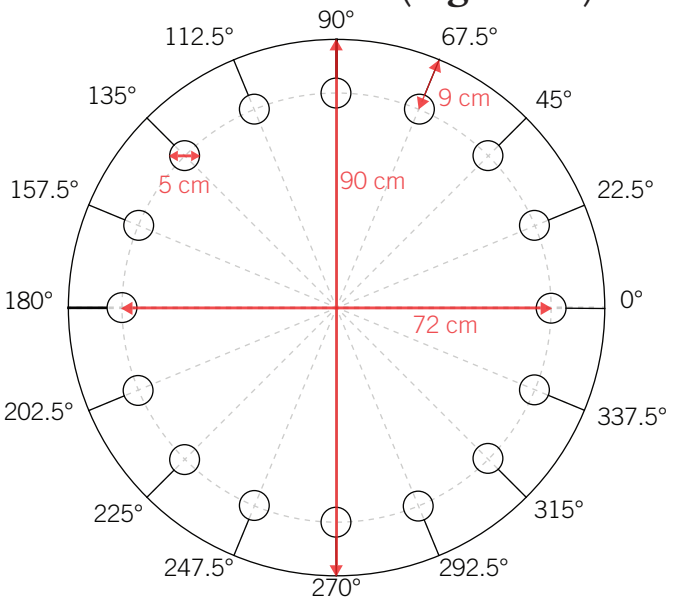

Figure 11 | Apparatus measurements for the Barnes maze. A circular platform with holes along the circumference.

floor of the covered holes.

A number of distal visual cues were present in many different positions and distances from the maze in the recording room. These were not moved throughout the experiment.

The start box was an octagonal opaque plastic box with an open roof (~ 16 cm ø, 25 cm tall) which could be separated in the middle so that it could be easily removed without obstructing the optic fibers. The escape box was a green elastic polypropylene container (Coline, 14.5 × 9.4 cm, 7.5 cm tall) with a tiny staircase inside, placed under the target hole. The elasticity let the box be fastened to or removed from small ledges on the underside of the maze without any chance of pinching the animal. A camera (Bosch LTC0355) in the ceiling was centered above the maze and a single incandescent bulb (40 w) was placed next to the camera. Again, a system of weighted pulleys in the ceiling made sure optic fibers could move effortlessly in all spatial dimensions at the level of the maze.

1.11.2.2. Behavioral procedure

All mice were used in the object recognition experiments before they were part of the Barnes maze experiment.

The purpose of this task was to find the escape box beneath the target hole and enter into it. To control for location preference the mice were randomly assigned to one of two target holes (at 180° or 65.5°) which were kept constant for each respective mouse.

Before each session, the escape box was filled with some cake sprinkles (Dr. Oetker Mix) and some cotton from the nest of the mouse. It was then placed in the housing of the mouse and left there for 10-15 minutes to habituate the animal to the escape box.

Prior to the experiment, all mice were habituated to the maze and able to explore freely for 5 minutes before they were guided into the escape box, unless they had already climbed into it.

The experiment was done over 6 days, excluding habituation (**Figure 12**). On each day, the mice were submitted to 6 trials with ~5 minute wait in between trials. In all sessions, the mouse was first placed in a start box at the center of the maze. The start box was removed after 10 seconds and the mice could explore freely. During the first 4 days, referred to as spatial

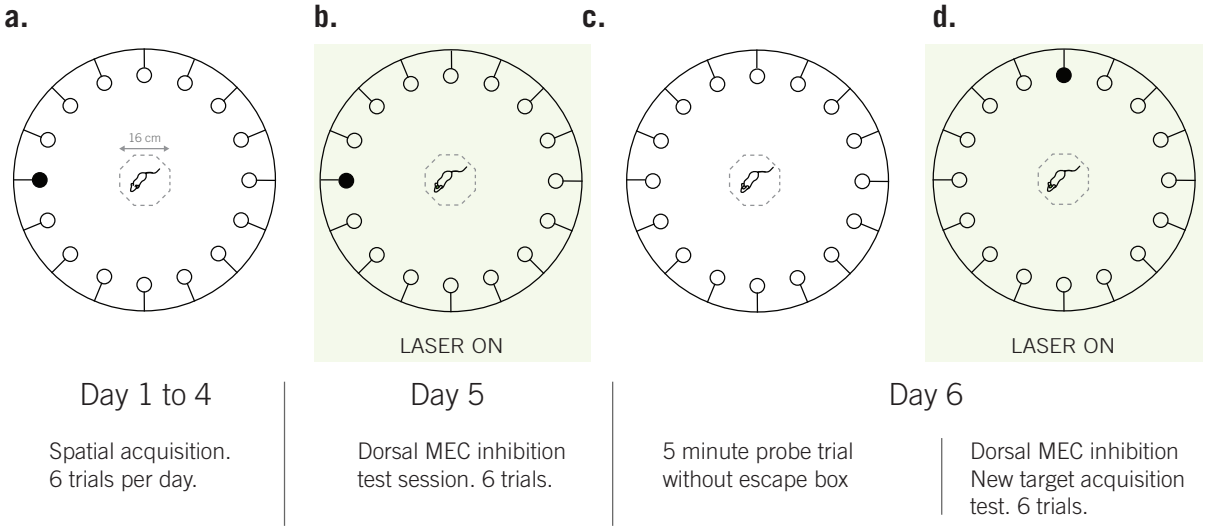

Figure 12 | Session layout for the Barnes maze experiment. a) Spatial acquisition sessions. Day 1 to 4 the mice were submitted to 6 trials per day without laser inhibition. b) Test session. On day 5 the mice were submitted to a test session with the laser turned on. c) On day 6, the mice were first submitted to a 5 minute probe trial without laser. d) On day 6, after the 5 minute probe trial, the mice were submitted to 6 trials with the laser turned on and the target hole at a new location 90° offset from the original target hole.

acquisition sessions, the mice learned where the target hole was located. On day 5 the target hole was still in the same location, but the laser was turned on for the last 5 trials (inhibition test). Laser stimulation began from the moment the mouse was placed in the start box.

On day 6, a probe trial was performed with the escape box removed, all the holes closed, and without photoinhibition. The mice were allowed to explore freely for 5 minutes until the escape box was placed under the previous target hole so that the mouse could escape.

5 minutes after the probe trial, the mice went through 6 more trials with the laser turned on (new target test), but with the target hole in a new location 90° offset from the target location of the preceding sessions (180° to 90°, 65.5° to 202.5°).

In between all trials the maze was washed with 70 % ethanol, and was rotated semi-randomly according to a predetermined pattern to minimize the number of times the same hole on the floor of the maze overlapped with the target hole position. The escape box was cleaned thoroughly with soap and water then 70 % ethanol before the start of each session, and with 70 % ethanol in between trials.

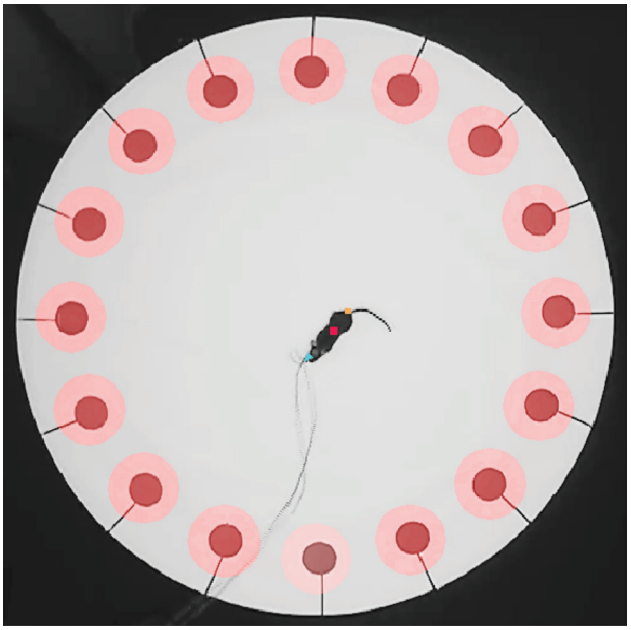

Figure 13 | Hole zones defined in the Barnes maze experiment. Each zone is 10 cm ø, covering 1.23% of the total area of the maze. Each hole zone is overlaid in red. The nose-point, body, and tail, was tracked at each time-point (25 fps). When the nose=point of the mouse enters a hole zone, the time-point of entry is registered. A subsequent visit to any particular hole is counted as only one visit in regards to strategy and error-calculations.

Figure 14 | (Below) Examples of each type of strategy used in the Barnes maze experiment.

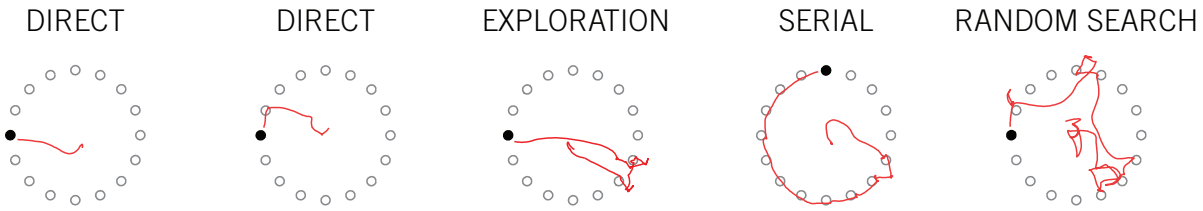

1.11.3.3. Data analysis

All trials were recorded and analyzed offline. Ethovision XT 8.5 was used to track the behavior of the mice, and to define a 10 cm ø hole zone to track the visits to each hole (**Figure 13**). Custom MatLab scripts were made to compute all behavioral variables from the raw data files output from Ethovision.

Several behavioral measures were analyzed: Velocity (cm/second), path length, number of errors, angular deviation, and the strategy the mouse used to find the target hole.

The number of errors for one trial was defined as the number of hole zones the mouse visited before reaching the target hole.

The angular deviation in a trial was defined as the lowest number of holes along the circumference from the first hole visited to the target hole (difference in units × 22.5°).

The strategy used in a trial was defined by the number and sequence of the visits to the hole zones until the mouse reached the target hole. Four types of strategies were defined (**Figure 14**). Direct strategy: If the mouse

ran directly to the target hole without visiting any other hole zones first, or visits less than three adjacent holes before the target hole. 2) Exploration strategy: If the mouse goes out in a particular direction, but then turns and uses the direct strategy as the first cross over the maze. 3) Serial strategy: If the mouse went out and first visited a closed hole more than 2 holes away from the target hole, then ran along the holes of the maze looking for the target hole. 4) Random search strategy: If the mouse searched holes in a pseudorandom sequence, often by combining a serial strategy with crosses to seemingly random locations around the maze. The direct, serial and random strategies are typically used in Barnes maze experiments (Barnes, 1979). The direct strategy is considered spatial, while the latter two are considered non-spatial. Sometimes the mice would go out in one direction, then turn and go directly for the target hole, using a spatial direct strategy, which led us to add the exploration strategy.

1.12. RESULTS

Mice initially used a serial approach to solving the task but gradually shifted to using a direct approach (**Figure 17**). When the mice were asked to find a new location (Session 6), they returned to using a serial approach, rather than a direct approach.

When the laser was turned on, the experimental group increased their running speed (**Figure 15 a, c**). This is similar to the averaged increased running speed observed in HCN1 knockout mice, which also lack the smallest grid scales (Giocomo et al., 2011). Because of this increase in speed, we focused our analyses on the number of errors made rather than latency effects.

The number of errors made between the two groups was not significantly different during session 5 as determined by a MANOVA ($F = 1.01$, $P = 0.623$) (**Figure 15 b, d**). No significant differences were observed between groups in measures of angular deviation.

After the inhibition test, mice were tested on 5 minute a probe trial with no escape hole. During this trial, both experimental animals and control animals more frequently visited the hole zone where the target hole had previously been located [experimental group: non-target(5.8±0.75), target(12.87±1.2), $t(3)= 5.89$, $P = 0.0098$] [control group: non-target(5.34±0.14), target(19.8±2.14), $t(3)=6.3$, $p=0.008$] (**Figure 16**). In the

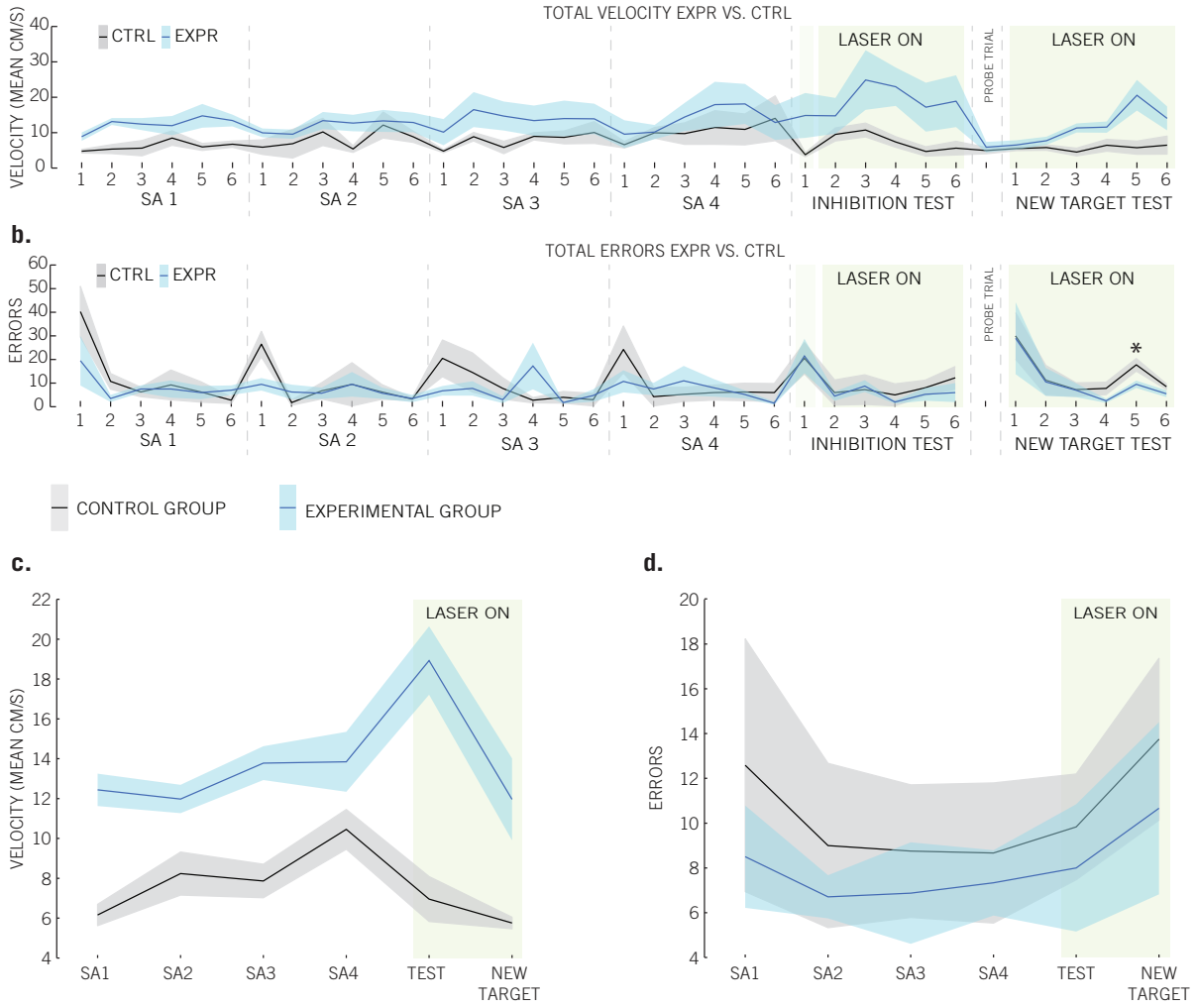

Figure 15 | Velocity and error statistics (mean ± sem). a) The mean velocity for each trial. b) The mean errors for each trial. c) Mean velocity of sessions, without the probe trial. d) Mean errors of sessions. Experimental group data represented in blue, control group data represented in black.

probe trial, three out of four control mice used a direct strategy with no errors before reaching the previous target hole. However, only one experimental mouse did the same. This difference in strategy was not significant in a X^2 [Pearson X^2(2, N=8)=2, p=0.157] but it should be noted that the number of animals is small.

Interestingly, in the new target test, mice switched back to using a serial approach to find the hole (**Figure 17**). During this probe, experimental mice made fewer total errors before entering the hole compared to control mice during the later trials (new target test trial 5 mean error Control = 17.5±2.66, Experiment =9.5±1.55 , Trial 5, F=7.18, P < .05). Tracking data

for each mouse can be reviewed in **Figure 18**, and **Figure 19**.

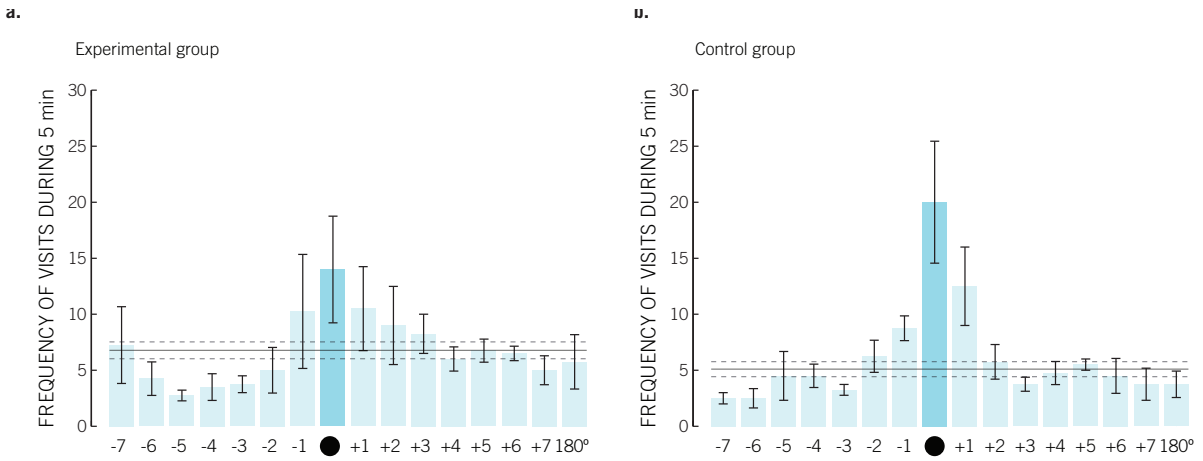

Figure 16 | Frequencies of visits for the holes in the no target probe test. The previous target zone (black circle) and holes in clockwise direction (+) and counterclockwise direction (-) from the previous target hole, for the experimental group (a), and the control group (b).

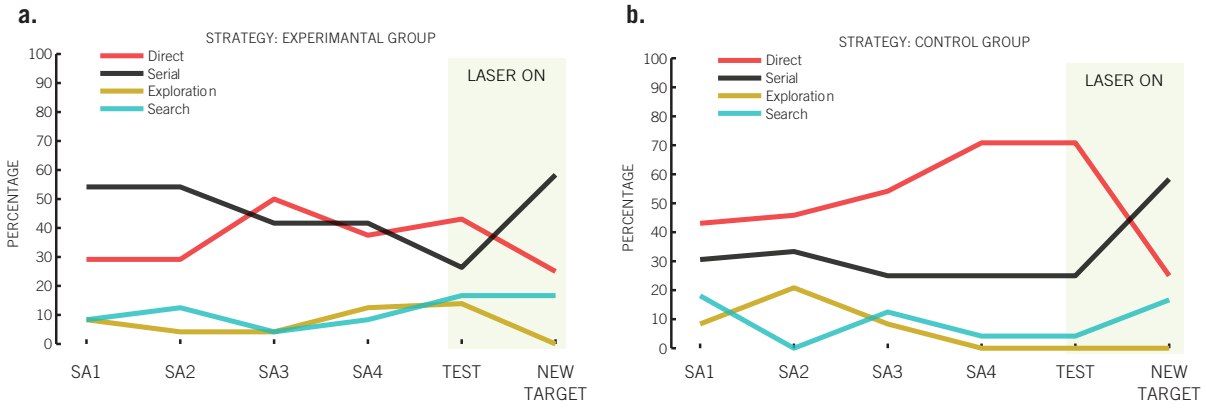

Figure 17 | Strategies used in the Barnes maze experiment. a) Experimental group. b) Control group.

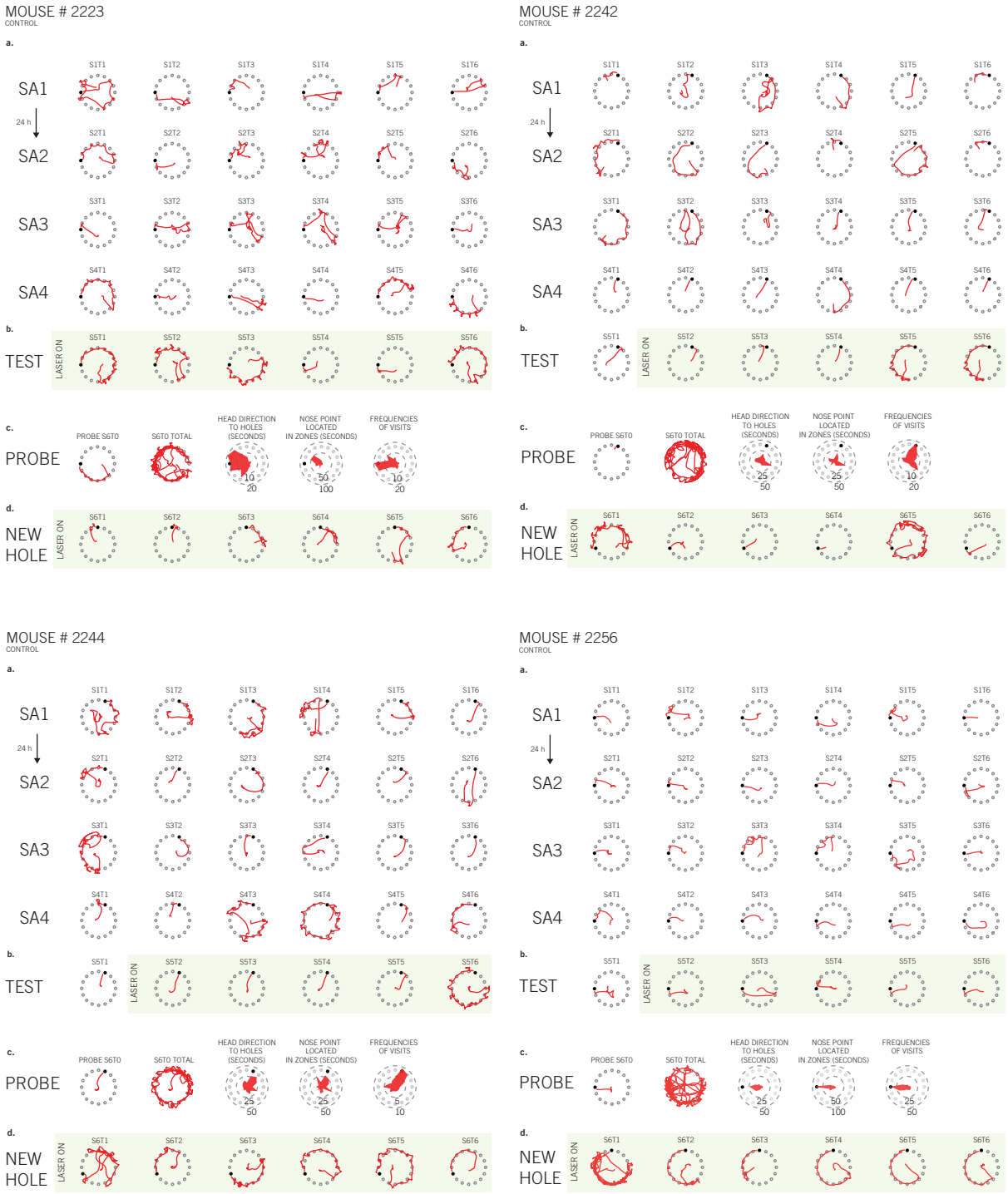

Figure 18 | Tracking data for each trial for the control group. a) Spatial acquisition (SA) sessions. b) Test session, with hole in the same position. c) 5 minute probe trial. d) New target test session.

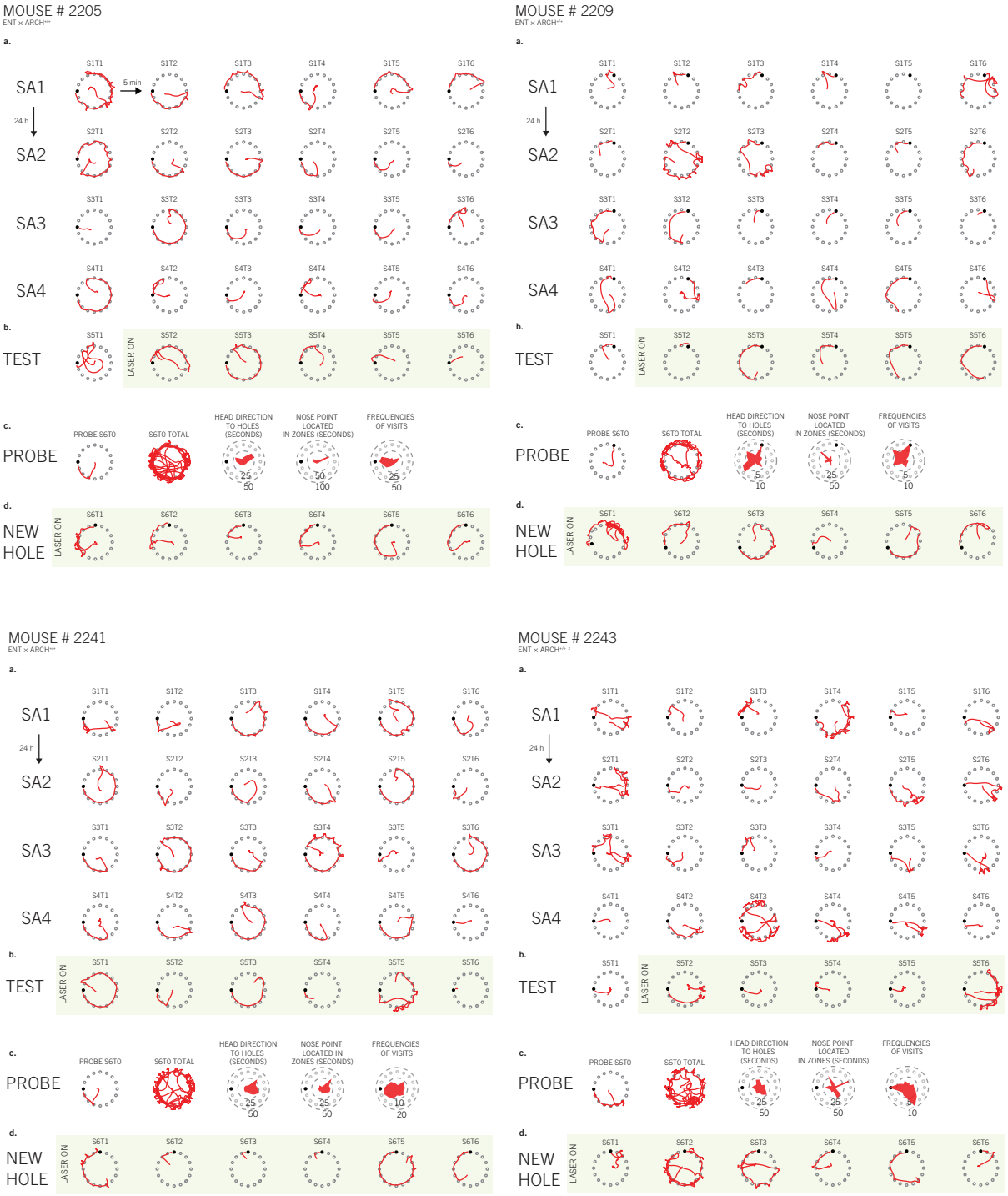

Figure 19 | Tracking data for each trial for the experimental group. a) Spatial acquisition (SA) sessions. b) Test session, with hole in the same position . c) 5 minute probe trial. d) New target test session.

5. RADIAL MAZE SPATIAL DELAYED-NON-MATCH-TO-SAMPLE CHOICE EXPERIMENT

The radial maze was built to be uniform and without discernible visual cues to help navigation. We wanted to see if the mice could remember which direction it came from based on idiothetic cues in an allothetically uniform environment after being delayed for a short period of time. We were also interested in determining If there was a difference in the ability of the mice to complete the task successfully when the goal arm is far from the start arm (three arms away, 67.5 degrees) or close to the start arm (the arm next to the start arm, 22,5 degrees) in mice with inhibited dorsal MEC activity. We chose to use a non-match-to-sample task in the radial maze, where after entrapment the mouse was given the choice of either moving into the arm it came from or moving into the only other open arm, the target arm, which contained a hole with an escape box and some cake sprinkles as reward.

1.13. METHODS

1.13.1.1. Apparatus

The apparatus was an enclosed 8-arm radial maze (32.5 cm long arms , 6 cm wide, 20 cm tall, with a 15 cm ø central area) (**Figure 20**). All parts of the maze were built with identical modules such that no part of the maze contained distinguishable visual cues. The radial maze was placed on top of the circular platform described in the Barnes maze experiment, such that the holes of the Barnes maze were located at the end of each arm. The end wall of each arm could be detached so that the escape box with the animal could be removed with the optic fibers connected. A detachable door was located at the entrance to each arm. The maze was surrounded by dark blue curtains from ceiling to floor in the last part of the experiment. Two lamps in the ceiling, one on each side of a centrally placed video camera, were configured to provide uniformly distributed soft light reflecting off the white ceiling to the maze to prevent differences in shadows falling in each arm of the maze.

To trap the animals in the centrum of the maze, we used a tube of black rubber (14 cm ø, 40 cm tall) open on top. It was separable into 4 parts, all with

magnetic bands along the edges so that when closed the parts aligned smoothly. The inside of the tube was covered with a black plastic sheet, also covering the magnets, to create an even surface.

The escape box was the same as described in the Barnes maze experiment.

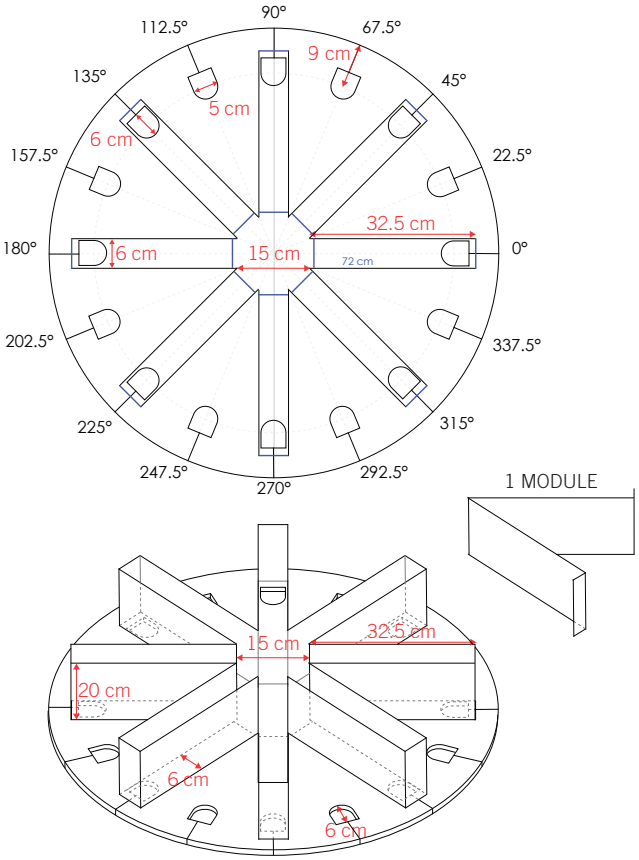

Figure 20 | Apparatus measures for the radial maze experiment.

1.13.2.2. Behavioral procedure

Before the experiment started, the mice were habituated to the maze and the escape box, as in the Barnes maze experiment.. The escape box was placed in the home cage of the mouse with a bit of cotton from its nest and some cake sprinkles (Dr. Oetker Mix). The mice were allowed to explore the escape box until they seemed comfortable (climbed in and out of the box, sat in the box and ate candy) for ~10-15 min. The escape box containing the mouse was lifted from the home cage and placed under a hole in an arm of the maze, making it possible for the mouse to climb out into the maze and explore. Two arms were open at 67.5 degrees between the arms. When the mouse returned to the escape box, the habituation trial was considered to be over.

Every test day, each mouse tested ran 10 trials.

The mice were connected to the optic fibers just prior to the trials. The fibers were reconnected if they got tangled, otherwise left connected until the end of the last trial.

Before a trial began only one arm was opened, the start arm. The mouse was placed in the center of the maze. After the mouse had explored the start arm, the mouse was trapped upon returning to the center of the maze. While the mouse was trapped, the maze was rotated such that the start arm

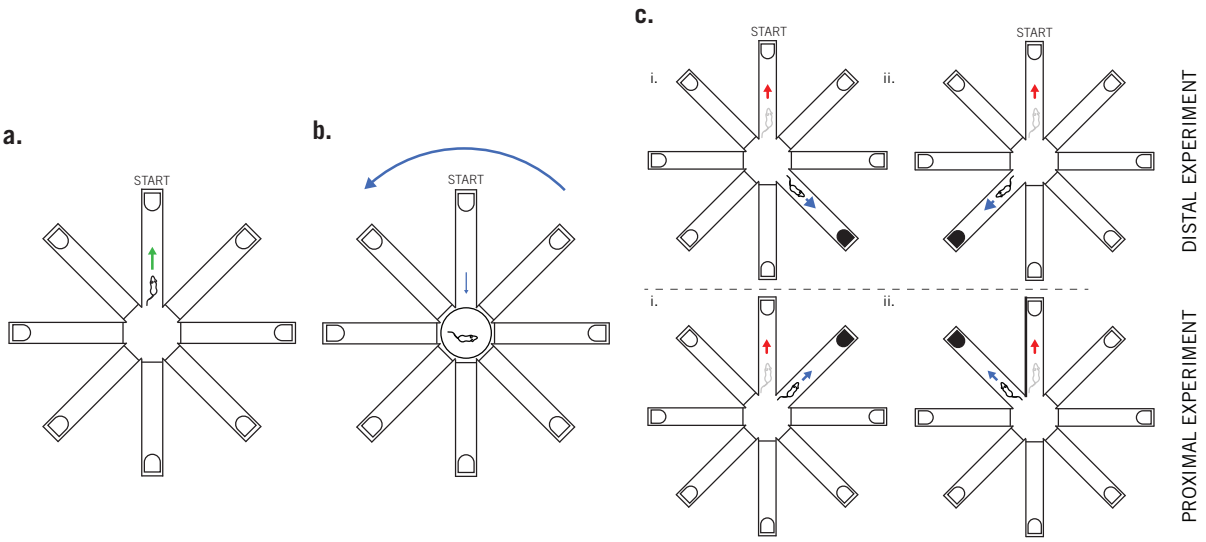

Figure 21 | Radial maze delay non-match-to-sample single trial layout. In each trial of this experiment, first a) the mouse is placed in the middle of the maze by hand and may explore one single open arm. b) When the mouse returns to the center of the maze, we trap the mouse in a container and wash the maze with 70% ethanol. After the first 6-7 training sessions the arms of the maze are rotated in every following trial, while the container and the floor remain stationary. c) To assure that the mouse does not simply learn to turn left or right, we randomly assign 50 % of the sessions with the open target arm either on the left or the right side of the start arm. The target arm has an open hole down to an escape box containing a few cake sprinkles as a reward. We then remove the container and let the mouse explore. If the mouse first reenters the explored start arm the trial is counted as a wrong choice. If, instead, the mouse first enters the unexplored target arm, the trial is counted as a correct choice.

contained new walls, and one more arm, the target arm, was opened containing the hole with the escape box. The floor of the start arm as well as the target arm and an additional random arm was cleaned with 70 % ethanol to remove odor cues before the entrapment tube was removed. The entrapment lasted ~30 seconds. If the mouse returned directly back to the start arm, the trial was counted as an error. If instead the mouse went to the target arm, it was counted as correct choice (**Figure 21**).

In between trials the mouse was placed into its home cage outside the curtains surrounding the recording area, as a reward for completing the trial. Here, the mice were safe and happy, whereas the transport box, where the mice were located during the connection of fiber implants, seemed to cause stress in some mice.

In the distal version of the task, the target arm was always 67.5 degrees away from the start arm. In the proximal version, the target arm was always 22.5 degrees away from the start arm. In both versions of the task, the target arm was placed either to the left of to the right of the start arm.

In the protocol, the mice were to be trained on the distal version 10 trials each session until they got correct choice on 8 out of 10 trials two days in a row. We then turn the laser on the next two ten trial sessions. After which the same procedure was to be performed in the proximal version.

Cake sprinkles were left in a bowl without a lid for several days for some of the aroma to dissipate. A few cake sprinkles were placed in the escape box between each trial.

To control and randomize the possible unintended cues of the environment, the modules of the maze were shuffled randomly at the start of the day, so that the wall on one side of the arm was different from the corresponding wall the previous day. The start arm and corresponding target arm was changed every trial, so that the possible use of cues in the ceiling for navigation, like camera and lights, would be difficult.

If the mouse spent more than 20 seconds in the wrong arm a wiggled finger above the mouse, or a gentle touch of the mouse's tail, made the mouse move towards the target arm.

The first two training sessions were done without fibers connected. The first six training sessions were done without pulled curtains. The first six or seven training sessions were done without rotating the maze, depending on which dates the mice were trained. After the 7th session the holes were extended in the radial direction by one centimeter, to ease the entry.

The rest of the training sessions and the test sessions were with the rotation in the protocol, the curtains closed, and the extended holes.

The last two sessions (10 + 10 trials) before the inhibition trial was done on the same day with a 15 minute between sessions interval. The two sessions with laser inhibition was also done on the same day (10 + 10 trials) with 15 minutes in between sessions.

1.13.3.3. Data analysis

All trials were videotaped and reviewed later. Each trial was counted either as a wrong or as a correct choice based on which arm the mouse first entered after being trapped. The criterion for 'entering an arm' was moving with the nose point more than 5 centimeters into the arm. If the trial was completed as correct choice or wrong choice was done by eye by the experimenter upon review of the recorded trials. Trials with irregular events

were exempt from the analysis, e.g. if the fiber got stuck, or the mouse found an eyelash to snack upon. Test sessions (of 10 trials) with fewer than 7 trials completed without irregular events were exempt from the analysis, e.g., if the mouse displays very heightened stress levels or got injured the trials were discontinued that day and the mouse returned to its home cage.

The results for the two last training sessions (done one the same day) before the test sessions were collapsed to one and the same was done for the test sessions. X^2 tests were done to see if the observed choices were different from the expectancy of what you would observe by chance (50 % correct).

1.14. RESULTS

The eight arm experiments were done over a two months period. Due to technical complications and time consuming protocol the mice were trained on average every 3.5 days, with 10 trials each test day. 5 out of the total 170 (10 trial) test sessions (2.9%) were exempt from analysis, all in the early days of training. 20 out of the total 1746 trials were exempt from analysis for experiment error (1.14%).

None of the mice reached the criterion of at least 80 % correct two sessions in a row, and by initial assessment the mice in general did not seem to improve significantly over the course of the experiment. The experiment was cut off after two months due to time-restrictions on the project.

In the distal training sessions, the control group chose correct 56.84% of the time (374/658 trials), and the experimental group chose correct 54.07% of the time (272 /503).

Comparing the training sessions before starting the turning of the maze and the ones after, the control group chose correct 59.52% (136/336 trials [X^2(1,N =336)=12.19, p < 0.001]) of the time before and 54.03% (174/322 trials [X^2(1,N=322)=2.1, p =0.147]) after (excluding mouse # 2244, 55.01% (148/269 trials [X^2(1,N=269)=2.71, p=0.1]) correct before to 52.1% (137/263 trials [X^2(1, N=263),p=0.498]) correct after).

In the two last sessions before the laser, on average the controls chose correct 59.6 % (59/99 [X^2(1, n =99)=3.646, p=0.056]) of the time, and the experimental group 49.4 %(39/79 [X^2(1,n=79)=0.01,p=0.91]) of the time. Both close enough to be expected by chance (**Figure 22**) .

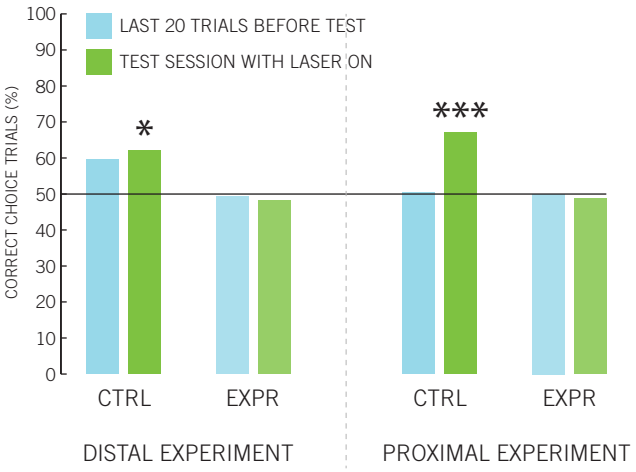

Figure 22 | Comparison of training and test sessions in the radial maze experiment. The percentage of correct choice trials in the last twenty trials before the test session with laser turned on (in blue), and the percentage of correct choice trials in the test sessions (in green), for the distal experiment, and for the proximal experiment. Asterisks added show results from X2 tests to check if the results deviated from random choice (50 % correct choice) (*, $p < 0.05$; **, $p < 0.001$).

The experimental group succeeded in 56.9% of the trials (151/265 trials) before and 50.84% (121/238 trials) after the start of maze rotation in the protocol. Separating out results from before and after the beginning of rotating the maze during trials, the experimental group chose more correct before [X^2(1,N=265) = 5.166, P = 0.023], than after [X^2(1, N=238)=0.67, P=0.795] rotating the maze was implemented. Possibly, some of the mice might have been using intramaze cues to navigate before the rotating was implemented.

In the distal inhibition trials the control group chose correct 62% of the time (62/100 trials [X^2(1,n=100)=5.76,p=0.016]) , and the experimental group chose correct 48.1% of the time (38/79 trials [X^2(1,n=79)=0.11,p=0.736]).

In the Proximal protocol the control group chose correct 50.5% of the time (50/99 [X^2(1,n=99)=0.01, p=0.92]) in the two training trials, and 67% (67/100 [X^2(1,n=100)=11.56,p=0.001]) correct in the laser trial. The experimental group chose 50% (40/80 trials [X^2(1,n=80)=0, p=1]) correct in the training trials and 48.75% (39/80 [X^2(1,n=80)=0.05, p=0.823]) correct in the laser trial.

The tendency for the control group to increase in the correct choices during trials with laser on is hard to explain. In the distal testing, the average number of days between the last training and tests were 4.6 for the control group, and 5.5 for the experimental group, while on the proximal testing the average number of days in between testing was 6 for the experimental group. This difference can not explain the results as there is no negative

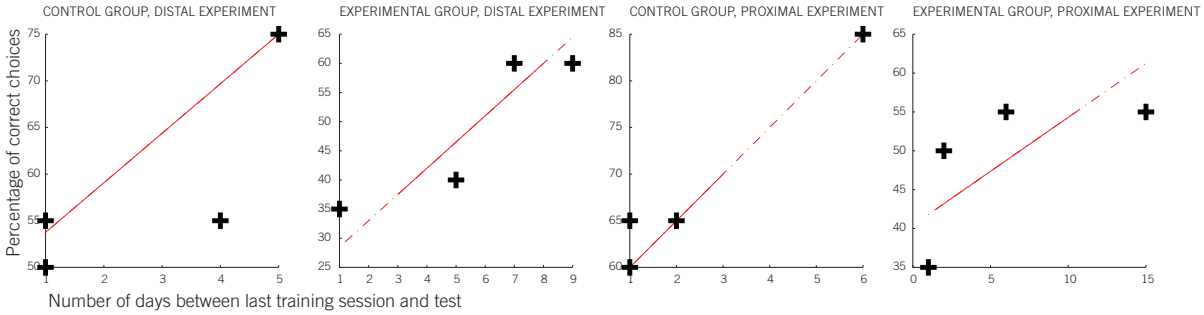

Figure 23 | Correlation plots for the number of days in between last testing and percentage of correct choices.

correlation between number of days between tests and retention (**Figure 23**). An alternative interpretation might be that the protocol without food restriction was not sufficient enough to provoke consistent correct choice behavior, while the addition of the laser might have startled the animals enough to make them try to escape. In this case, the experimental group with inhibited activity in the dorsal MEC might have problems choosing correctly, while the control group less so.

The mice had already been trained in the same room to navigate by relying on distal visual cues. Doing the two experiments in reverse order could be beneficial.

In one of the training sessions of mouse 2244 the light bulb broke in one of the lamps in the ceiling, and distinct shadows took form on the floor of the maze, cast differently in each arm. Interestingly, in this session, the mouse completed all trials with correct choice, suggesting the task with navigational cues from the shadows might be completed more readily.

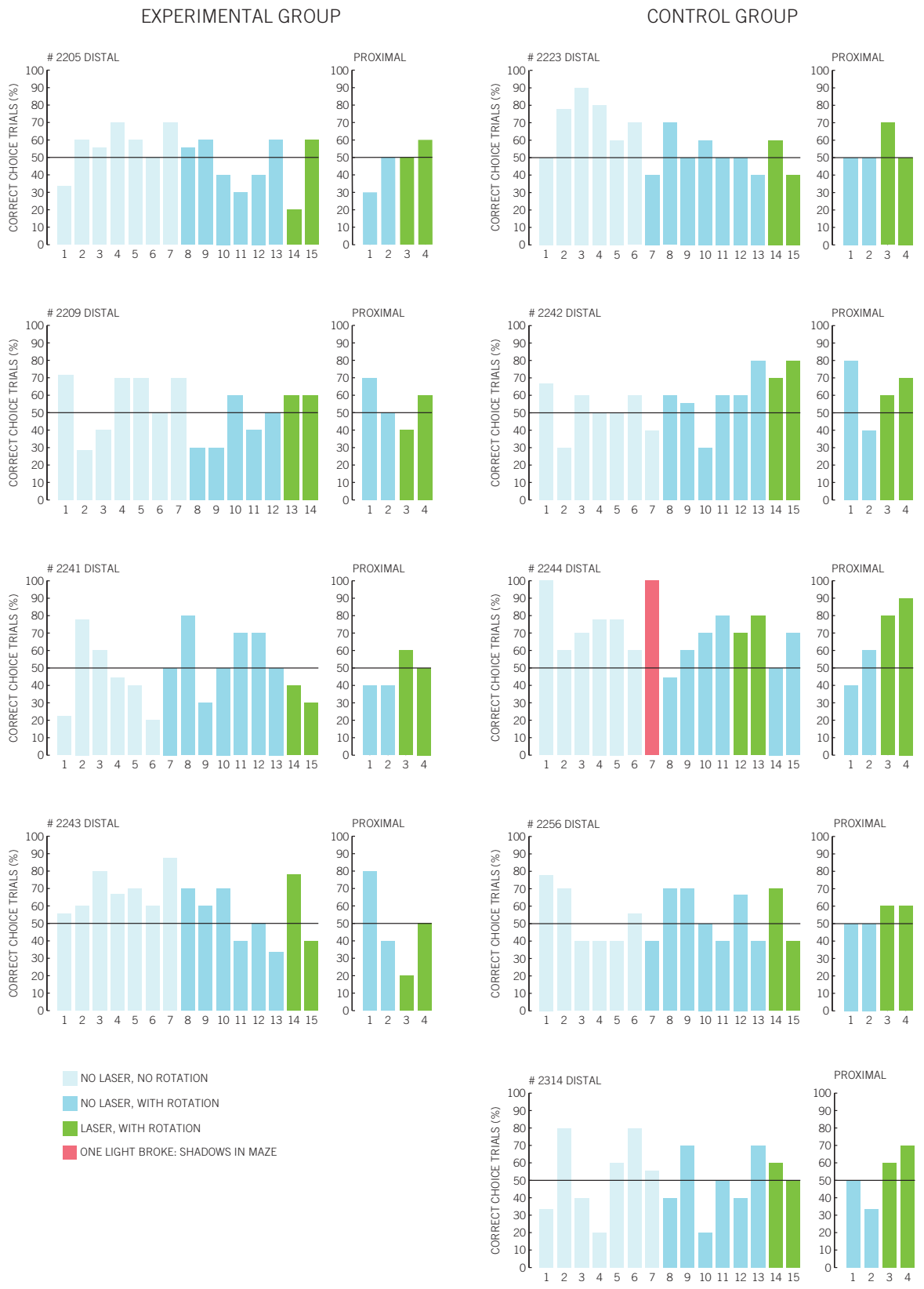

Figure 24 | Percentage of correct choices for each mouse in each session of the DNMS experiment.

6. DISCUSSION

Earlier studies on the firing properties of principal cells in the medial entorhinal cortex (MEC) as well as lesion studies suggest the area plays a major role in the processing of spatial memory and navigation (Hafting et al., 2005; Steffenach et al., 2005; Van Cauter et al., 2013). The main goal of this project was to investigate how the topographical organization of the grid scale along the dorsoventral axis of the MEC contributes to memory and navigation. In this endeavor we used a transgenic mouse line expressing archeorhodopsin selectively in layer II of the MEC. We disrupted activity bilaterally in a subset of the principal cells within the dorsalmost [~0.7 mm] MEC, during crucial moments of several behavioral tasks where varying degrees of accuracy in spatial processing were essential for successful completion. We found that mice were significantly impaired on spatial tasks where it was not possible for the mice to use an alternative non-spatial strategy. The three behavioral paradigms utilized in this study were an object recognition experiment, a Barnes maze experiment, and a delayed non-match-to-sample spatial task designed to test idiothetic integration.

First, we examined the mice on an object recognition task. The initial goal of this task was to compare proximal versus distal spatial and non-spatial encoding. We hypothesized that mice with photoinhibited dorsal MEC would perform poorly on spatial versions of the task and that their performance would be worse when the task involved a small (proximal) change compared to a large (distal) change. We found that in the distal version of this task experimental mice were significantly impaired on the spatial versus non-spatial change. This raises the possibility that dorsal MEC is needed for either the identification or encoding of spatial schemas, consistent with previous lesion work (Steffenach et al., 2005). The mice were also unimpaired in the non-spatial change, consistent with previous lesion work (Van Cauter et al., 2013). It should be noted that the proximal version of the task proved very challenging for the mice and thus, future work could test variants of such a task to see if a less-challenging proximal version of the task could be developed. Nevertheless, in the proximal experiment, while both normal mice and sham operated mice did show a significant increase of exploration of the manipulated objects in both spatial and nonspatial change

after the manipulation, the experimental group did not display a significantly higher exploration time for the moved object in the spatial change. This suggests variants of such a task might give results. Furthermore, the results for the intact mice in this experiment suggest that they can learn spatial and non-spatial object recognition tasks when connected to optical fibers and these tasks could be utilized for future studies of learning and memory in mice.

Second, we examined the mice on a Barnes maze task. We hypothesized that the mice with photoinihibited dorsal MEC would perform with less spatial precision than controls. If the ability of detailed spatial orientation was altered by inhibiting the smallest scale grid network, the mice would be left with a more general notion of where the target hole was located, accumulating more errors and showing a greater angular deviation than controls. The results showed that the experimental mice did not perform statistically differently from the controls during photoinhibition when they navigated to a familiar target hole. Earlier lesion studies show that dorsolateral entorhinal lesions lead to a nonfunctioning retention of previously learned spatial information while new information can be learned more readily (Steffenach et al., 2005). The results from this test combined with the object recognition results might seem to show the opposite, but this is not the case. On the inhibition test day, most of the mice first ran a test session without inhibition, and then proceeded to run the trial five more times, corroborating the finding that the mice can still learn in a test with a spatial goal despite inhibition of a subset of the MEC grid cells. It is possible that the photoinhibited area of the MEC was too small to effectively disrupt such a heavily goal related task while provided with ample navigational cues. Alternatively, or in addition, neither the controls nor the experimental group performed exceptional during the test, and more pretest training might have led to a bigger difference between the groups. The experimental mice perform better than controls after a spatial change (new hole location) but this most likely results from a switch from a spatial to a nonspatial strategy they use to solve the task. If they were forced to use a direct strategy after the change in the hole location, the mice may have performed poorly.

Finally, we examined the mice in spatial delayed non-match-to-sample (DNMS) test, where spatial cues were removed such that the mice would have to rely on idiothetic cues to track their preceding movement. We hypothesized that disrupting activity in the entorhinal cortex during this task would impede the performance due to the areas probable role in path integration (McNaughton et al., 2006). The results indicate that the experimental mice did not show any sign of learning the task; the same was initially true for the sham operated controls. However, when the laser was turned on, the control group did better than expected by chance while the experimental mice still performed at chance level indicating the initial assessment might have been due to insufficient motivation. The results suggest that tests of a role for the layer II MEC cells in path integration could prove fruitful. The lack of positive baseline results in our experiment is a serious hamper to interpretation. And further experimentation using a similar task would need to refine the design to achieve good baseline results. Another problem with this task design is that the mice were forced to delay choice of the arm, such that a disruption of short term memory alone would produce the same results regardless of which types of cues the mice use to navigate by. In one session of this experiment, when a light bulb broke in the ceiling, shadows of different shapes on the floor of each arm provided a control mouse with ample intramaze cues to navigate by, and the mouse ran ten subsequent trials successfully before the experimenter noticed. This slipup might suggest that mice can navigate very well by integrating local cues compared to navigating by idiothetic cues alone in this type of task.

The inclusion of the use of optic fibers to the tasks was less trivial than expected. Of course, the objects selected for the object recognition protocols must be smooth enough to allow the fibers to glide along them unimpeded from all angles. One mishap in the object recognition protocol was the use of objects with reflective surfaces combined with the translucent dental cement implants. The light shines through the cement, and the mice might find renewed interest in reflective surfaces. This might have caused renewed interest in the unmoved object in the spatial condition of these experiments, and thus kept the discrimination ratio closer to 0 than would have been the case otherwise. In future experiments it is advisable to use

opaque implants to prevent this task dependent light as a possible confounding factor. The modification of the Barnes maze, including slits to channel the fibers upon removal of the mice did not affect the task, and can be included in further experiments. We used 5 cm ø holes on a 90 cm ø maze, which did work, but required extra preparation with the implanted mice, as they needed to learn how to enter without hinging the implant to the edge. Future studies should consider using larger holes which would also require a larger diameter of the circular platform to ensure the escape box can not be spotted readily by the animal. The experimenter's apprehension to causing discomfort to the animals might have affected the results; the use of stressors in these experiments was minimal. In the Barnes maze, the light source was not much brighter than a normal desk lamp, and the training of the mice to be picked up by the researcher might have affected their behavior. The idea behind combining the radial maze and Barnes maze was to prevent the use of food deprivation. The animals had ad libidum access to the food and water at all time. In combination with the soft light to prevent strong shadows this might have influenced the results on the spatial DNMS task.

Using optic fibers alone without simultaneous electrophysiological recording for feedback leaves a lot of uncertainty in terms of the extent of the inhibition. The extremely fragile fibers might break inside the implant without the experimenter knowing or incorrectly connected fibers on some trials might affect the results. Nevertheless, we took care to protect the implant and connections, and we assume the amount cells inhibited in this study is restricted to a plume shaped area of about 0.7 mm * 105µm ø directed from the tip of the fiber. Although some of the implants were located more anterior than intended, possibly inhibiting the transmission in the axons of a larger set of cells, the fibers directed at the MEC should disrupt firing in a limited subset of the dorsal MEC neurons. Yet, the amount of disruption in MEC activity was enough to debilitate the transgenic mice in object recognition with a spatial change within the spatial extent we tested the mice (< 90 cm2), and also possibly affecting the use of idiothetic cues for navigation. This raises the possibility that grid cells in the very dorsal portion of MEC might be important for successful spatial memory and

navgation after changes to the spatial environment. If the spatial resolution of the grid scale is as important for precise navigation as hypothesized, future probes should use tests with configurational changes in a larger spatial extent than was done in this study.

It is possible that small scale grid cells are particularly helpful when performing a spatial memory or navigation task after a spatial change. Stensola et al. (2012) indicated that when a familiar environment undergoes a geometric (spatial) change, the small scale grid cells are the only cells that retain the same scale. Larger scale grid cells often change their scale transiently to reflect the geometric change. Perhaps the inflexibility of the small grid cells after geometric changes to the environment support navigation or spatial memory under novel or changed spatial conditions.

7. REFERENCES

Amaral DG, Witter MP (1989) The three-dimensional organization of the hippocampal formation: a review of anatomical data. Neuroscience 31:571–591.

Barnes CA (1979) Memory deficits associated with senescence: a neurophysiological and behavioral study in the rat. J Comp Physiol Psychol 93:74–104.

Barry C, Ginzberg LL, O'Keefe J, Burgess N (2012) Grid cell firing patterns signal environmental novelty by expansion. Proc Natl Acad Sci U S A 109:17687–17692.

Barry C, Hayman R, Burgess N, Jeffery KJ (2007) Experience-dependent rescaling of entorhinal grids. Nat Neurosci 10:682–684.

Boccara CN, Sargolini F, Thoresen VH, Solstad T, Witter MP, Moser EI, Moser MB (2010) Grid cells in pre- and parasubiculum. Nat Neurosci 13:987–994.

Brun VH, Otnass MK, Molden S, Steffenach HA, Witter MP, Moser MB, Moser EI (2002) Place cells and place recognition maintained by direct entorhinal-hippocampal circuitry. Science 296:2243–2246.

Brun VH, Solstad T, Kjelstrup KB, Fyhn M, Witter MP, Moser EI, Moser MB (2008) Progressive increase in grid scale from dorsal to ventral medial entorhinal cortex. Hippocampus 18:1200–1212.

Clark BJ, Taube JS (2012) Vestibular and attractor network basis of the head direction cell signal in subcortical circuits. Front Neural Circuits 6:7.

Colgin LL, Moser EI, Moser MB (2008) Understanding memory through hippocampal remapping. Trends Neurosci 31:469–477.

Corkin S, Amaral DG, González RG, Johnson KA, Hyman BT (1997) H. M.'s medial temporal lobe lesion: findings from magnetic resonance imaging. J Neurosci 17:3964–3979.

Douglas RJ (1967) The hippocampus and behavior. Psychol Bull 67:416–422.

Dupret D, O'Neill J, Pleydell-Bouverie B, Csicsvari J (2010) The reorganization and reactivation of hippocampal maps predict spatial memory performance. Nat Neurosci 13:995–1002.

Fuhs MC, Touretzky DS (2006) A spin glass model of path integration in rat medial entorhinal cortex. J Neurosci 26:4266–4276.

Fyhn M, Hafting T, Treves A, Moser MB, Moser EI (2007) Hippocampal remapping and grid realignment in entorhinal cortex. Nature 446:190–194.

Fyhn M, Hafting T, Witter MP, Moser EI, Moser MB (2008) Grid cells in mice. Hippocampus 18:1230–1238.

Fyhn M, Molden S, Witter MP, Moser EI, Moser MB (2004) Spatial representation in the entorhinal cortex. Science 305:1258–1264.

Gener T, Perez-Mendez L, Sanchez-Vives M V (2013) Tactile modulation of hippocampal place fields. Hippocampus:"Accepted Article", doi: 10.1002/hipo.22198.

Hafting T, Fyhn M, Molden S, Moser MB, Moser EI (2005) Micro-

structure of a spatial map in the entorhinal cortex. Nature 436:801–806.

Hama H, Kurokawa H, Kawano H, Ando R, Shimogori T, Noda H, Fukami K, Sakaue-Sawano A, Miyawaki A (2011) Scale: a chemical approach for fluorescence imaging and reconstruction of transparent mouse brain. Nat Neurosci 14:1481–1488.

Han X, Chow BY, Zhou H, Klapoetke NC, Chuong A, Rajimehr R, Yang A, Baratta M V, Winkle J, Desimone R, Boyden ES (2011) A high-light sensitivity optical neural silencer: development and application to optogenetic control of non-human primate cortex. Front Syst Neurosci 5:18.

Hurst JL, West RS (2010) Taming anxiety in laboratory mice. Nat Methods 7:825–826.

Jezek K, Henriksen EJ, Treves A, Moser EI, Moser MB (2011) Theta-paced flickering between place-cell maps in the hippocampus. Nature 478:246–249.

Kelemen E, Fenton AA (2010) Dynamic grouping of hippocampal neural activity during cognitive control of two spatial frames. PLoS Biol 8:e1000403.

Langston RF, Wood ER (2010) Associative recognition and the hippocampus: differential effects of hippocampal lesions on object-place, object-context and object-place-context memory. Hippocampus 20:1139–1153.

Lavenex P, Amaral DG (2000) Hippocampal-neocortical interaction: a hierarchy of associativity. Hippocampus 10:420–430.

Lee I, Rao G, Knierim JJ (2004) A double dissociation between hippocampal subfields: differential time course of CA3 and CA1 place cells for processing changed environments. Neuron 42:803–815.

Leutgeb S, Leutgeb JK, Treves A, Moser MB, Moser EI (2004) Distinct ensemble codes in hippocampal areas CA3 and CA1. Science 305:1295–1298.

Lever C, Burton S, Jeewajee A, O'Keefe J, Burgess N (2009) Boundary vector cells in the subiculum of the hippocampal formation. J Neurosci 29:9771–9777.

Lever C, Wills T, Cacucci F, Burgess N, O'Keefe J (2002) Long-term plasticity in hippocampal place-cell representation of environmental geometry. Nature 416:90–94.

Marr D (1971) Simple memory: a theory for archicortex. Philos Trans R Soc Lond B Biol Sci 262:23–81.

McNaughton BL, Battaglia FP, Jensen O, Moser EI, Moser MB (2006) Path integration and the neural basis of the "cognitive map". Nat Rev Neurosci 7:663–678.

Mizuseki K, Royer S, Diba K, Buzsáki G (2012) Activity dynamics and behavioral correlates of CA3 and CA1 hippocampal pyramidal neurons. Hippocampus 22:1659–1680.

Moita MA, Rosis S, Zhou Y, LeDoux JE, Blair HT (2003) Hippocampal place cells acquire location-specific responses to the conditioned stimulus during auditory fear conditioning. Neuron 37:485–497.

Morris RGM (1981) Spatial localization does not require the presence of local cues. Learn Motiv 12:239–260.

Morris RGM, Garrud P, Rawlins JN, O'Keefe J (1982) Place navigation impaired in rats with hippocampal lesions. Nature 297:681–683.

Muller RU, Kubie JL (1987) The effects of changes in the environment on the spatial firing of hippocampal complex-spike cells. J Neurosci 7:1951–1968.

Naber PA, Lopes da Silva FH, Witter MP (2001) Reciprocal connections between the entorhinal cortex and hippocampal fields CA1 and the subiculum are in register with the projections from CA1 to the subiculum. Hippocampus 11:99–104.

O'Keefe J (1976) Place units in the hippocampus of the freely moving

rat. Exp Neurol 51:78–109.

O'Keefe J, Burgess N (1996) Geometric determinants of the place fields of hippocampal neurons. Nature 381:425–428.

O'Keefe J, Burgess N (2005) Dual phase and rate coding in hippocampal place cells: theoretical significance and relationship to entorhinal grid cells. Hippocampus 15:853–866.

O'Keefe J, Conway DH (1978) Hippocampal place units in the freely moving rat: why they fire where they fire. Exp Brain Res 31:573–590.

O'Keefe J, Dostrovsky J (1971) The hippocampus as a spatial map. Preliminary evidence from unit activity in the freely-moving rat. Brain Res 34:171–175.

O'Keefe J, Nadel L (1978) The hippocampus as a cognitive map. Walton Street, Oxford: Oxford University Press.

Parron C, Save E (2004) Evidence for entorhinal and parietal cortices involvement in path integration in the rat. Exp Brain Res 159:349–359.

Redish AD, Battaglia FP, Chawla MK, Ekstrom AD, Gerrard JL, Lipa P, Rosenzweig ES, Worley PF, Guzowski JF, McNaughton BL, Barnes CA (2001) Independence of firing correlates of anatomically proximate hippocampal pyramidal cells. J Neurosci 21:RC134.

Sargolini F, Fyhn M, Hafting T, McNaughton BL, Witter MP, Moser MB, Moser EI (2006) Conjunctive representation of position, direction, and velocity in entorhinal cortex. Science 312:758–762.

Save E, Nerad L, Poucet B (2000) Contribution of multiple sensory information to place field stability in hippocampal place cells. Hippocampus 10:64–76.

Schenk F, Morris RG (1985) Dissociation between components of spatial memory in rats after recovery from the effects of retrohippocampal lesions. Exp Brain Res 58:11–28.

Scoville WB, Milner B (1957) Loss of recent memory after bilateral hippocampal lesions. J Neurol Neurosurg Psychiat 20:11–21.

Skelton RW, McNamara RK (1992) Bilateral knife cuts to the perforant path disrupt spatial learning in the Morris water maze. Hippocampus 2:73–80.

Solstad T, Boccara CN, Kropff E, Moser MB, Moser EI (2008) Representation of geometric borders in the entorhinal cortex. Science 322:1865–1868.

Solstad T, Moser EI, Einevoll GT (2006) From grid cells to place cells: a mathematical model. Hippocampus 16:1026–1031.

Squire LR (2004) Memory systems of the brain: a brief history and current perspective. Neurobiol Learn Mem 82:171–177.

Steffenach HA, Witter M, Moser MB, Moser EI (2005) Spatial memory in the rat requires the dorsolateral band of the entorhinal cortex. Neuron 45:301–313.

Stensola H, Stensola T, Solstad T, Frøland K, Moser MB, Moser EI (2012) The entorhinal grid map is discretized. Nature 492:72–78.

Taube JS (1995) Head direction cells recorded in the anterior thalamic nuclei of freely moving rats. J Neurosci 15:70–86.

Taube JS, Muller RU, Ranck JB (1990a) Head-direction cells recorded from the postsubiculum in freely moving rats. I. Description and quantitative analysis. J Neurosci 10:420–435.

Taube JS, Muller RU, Ranck JB (1990b) Head-direction cells recorded from the postsubiculum in freely moving rats. II. Effects of environmental manipulations. J Neurosci 10:436–447.

Thompson LT, Best PJ (1990) Long-term stability of the place-field activity of single units recorded from the dorsal hippocampus of freely behaving rats. Brain Res 509:299–308.

Tolman EC (1948) Cognitive maps in rats and men. Psychol Rev 55:189–208.

Tolman EC, Ritchie BF, Kalish D (1946) Studies in spatial learning. I. Orientation and the short-cut. J Exp Psychol 36:13–24.

Van Cauter T, Camon J, Alvernhe A, Elduayen C, Sargolini F, Save E (2013) Distinct roles of medial and lateral entorhinal cortex in spatial cognition. Cereb Cortex 23:451–459.

Van Cauter T, Poucet B, Save E (2008) Delay-dependent involvement of the rat entorhinal cortex in habituation to a novel environment. Neurobiol Learn Mem 90:192–199.

van Strien NM, Cappaert NLM, Witter MP (2009) The anatomy of memory: an interactive overview of the parahippocampal-hippocampal network. Nat Rev Neurosci 10:272–282.

Witter MP (2011) Hippocampus. In: The Mouse Nervous System (Watson C, Paxinos G, Puelles L, eds), pp.112 – 138. London: Academic Press.

Yasuda M, Mayford MR (2006) CaMKII activation in the entorhinal cortex disrupts previously encoded spatial memory. Neuron 50:309–318.

Ziv Y, Burns LD, Cocker ED, Hamel EO, Ghosh KK, Kitch LJ, El Gamal A, Schnitzer MJ (2013) Long-term dynamics of CA1 hippocampal place codes. Nat Neurosci 16:264–266.

Supplementary material

S1 LASER INTENSITY MEASUREMENTS

Post mortem measurements of laser intensity coupling loss through implants embedded in the dissected cranium:

Animal ID	Left hemisphere implant output (input ~11 mW)	Right hemisphere implant output (input ~11 mW)
1884	1.3 mW★	2 mW★
2205	6.3 mW	0.3 mW★
2209	7 mW	2.5 mW
2223	7 mW	9 mW
2241	4.96 mW★	7.8 mW
2242	4.7 mW	8 mW
2243	7.24 mW	3.2 mW★
2244	7.4 mW	5 mW★
2256	7.92 mW	7.8 mW
2314	8.7 mW	7.4 mW

Table S1. Laser intensity measurements through optic fiber cannule implants after dissection. All values are approximate +- 0.5 mW with an input of ~11 mW. ★ denotes broken implants. The implant might have broken during dissection or earlier.

S2 HISTOLOGY OF EACH MOUSE

See next pages.

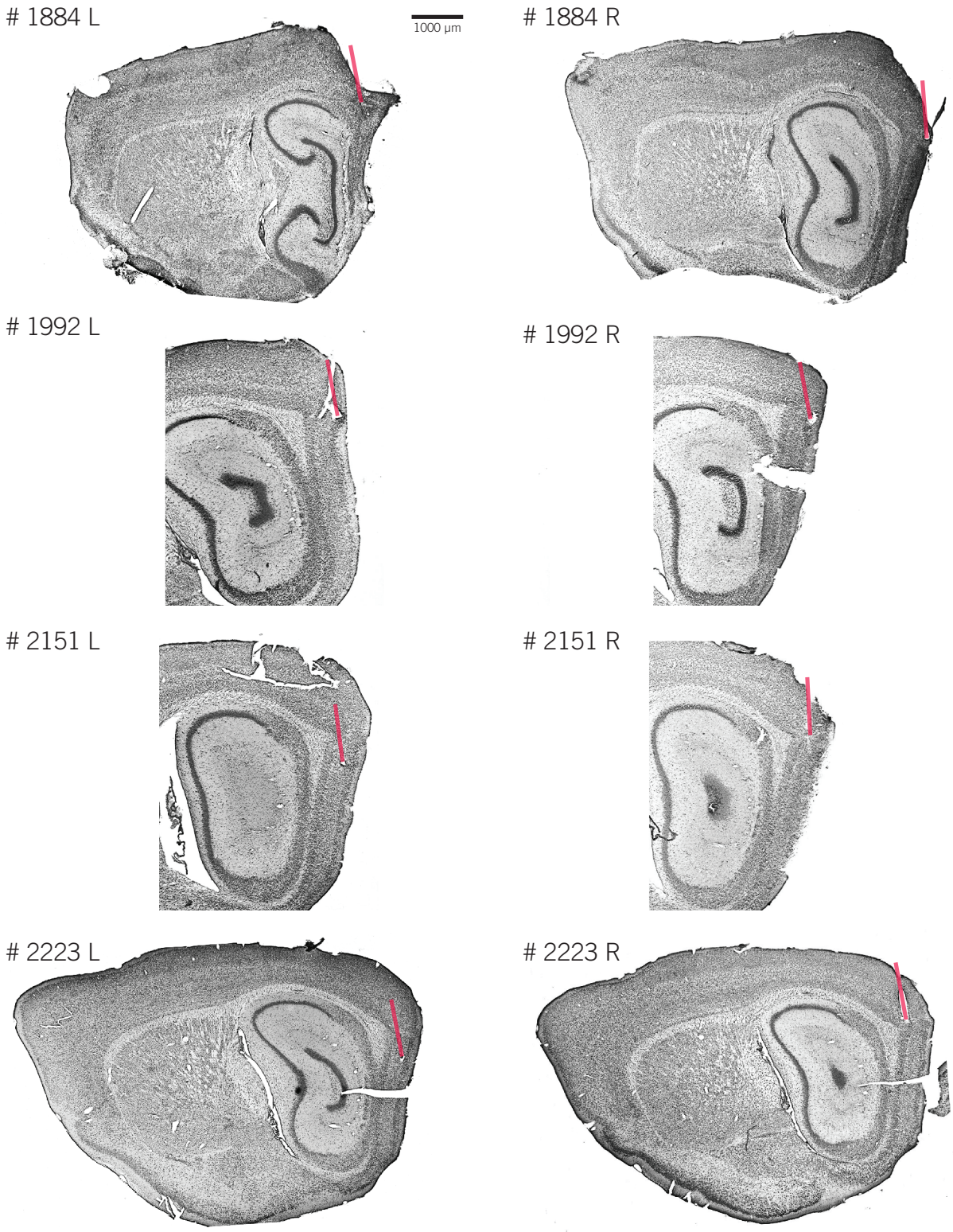

Sup. Figure 1 | ***Control group (sham operated) sagittal slices.*** Nissl stained. Red line indicates fiber implant track.

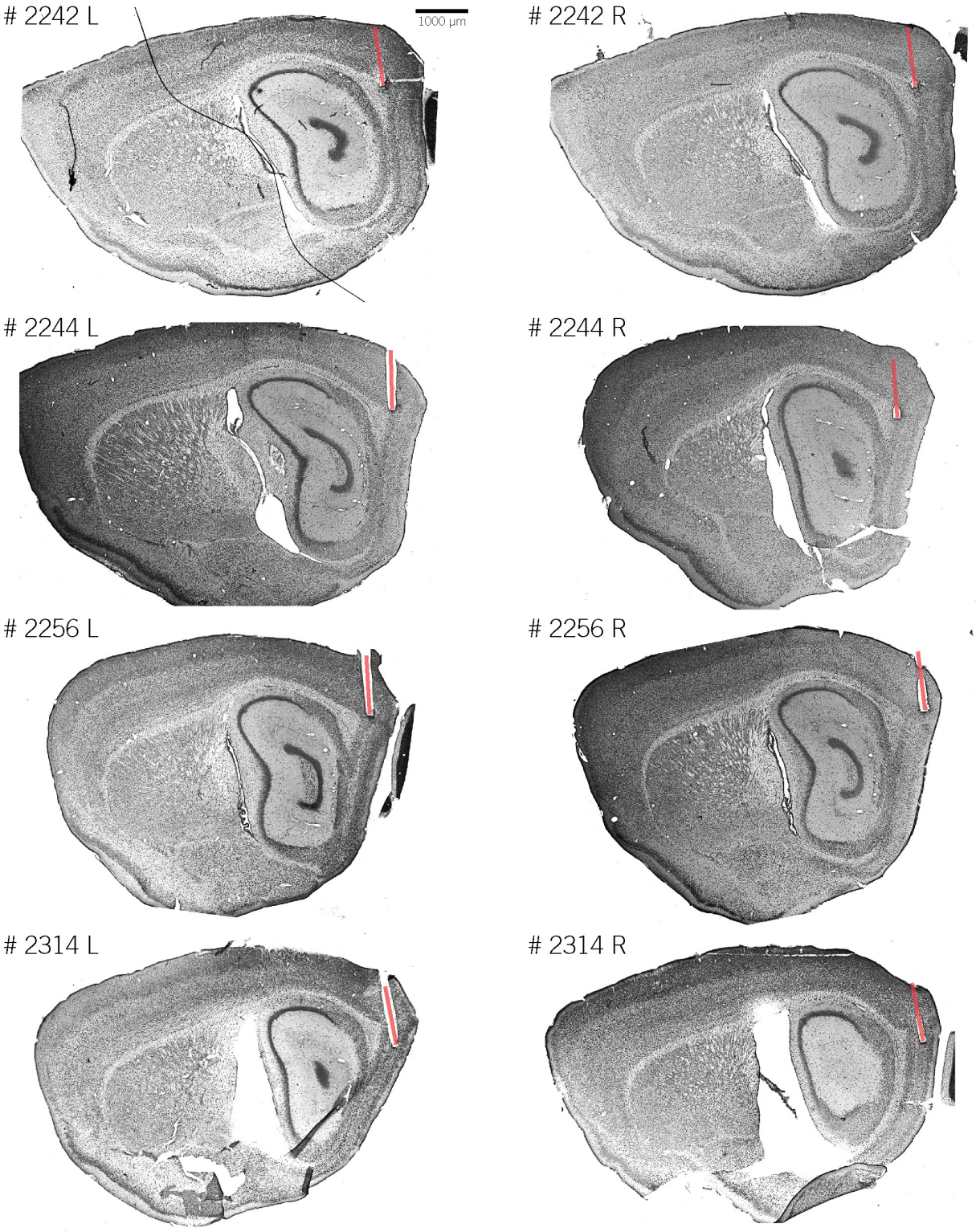

Sup. Figure 2 | Control group (sham operated) sagittal slices. Nissl stained. Red line indicates fiber implant track.

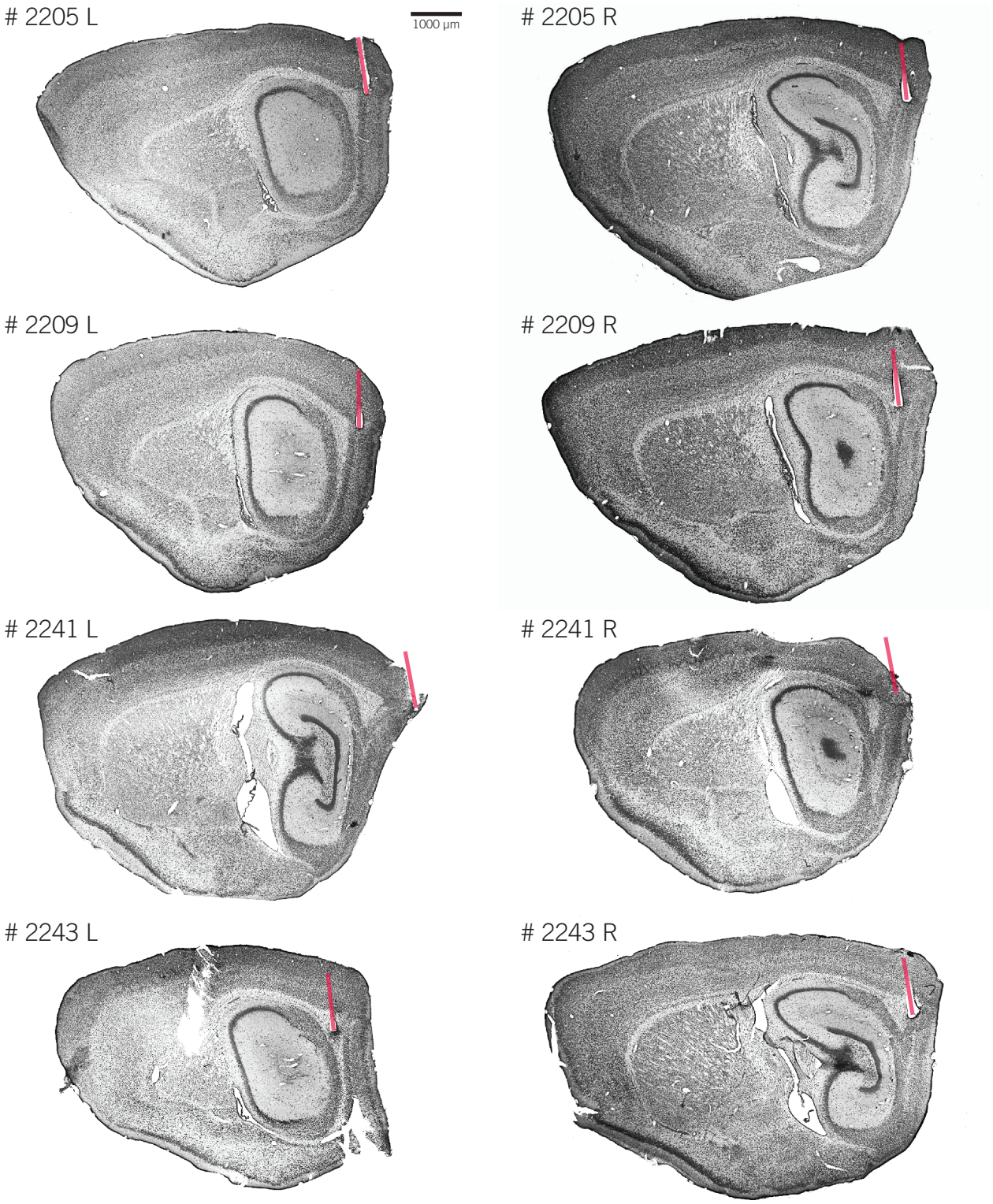

Sup. Figure 3 | E**xperimental group (ENT x ARCH+/+) sagittal slices.** Nissl stained. Red line indicates fiber implant track.

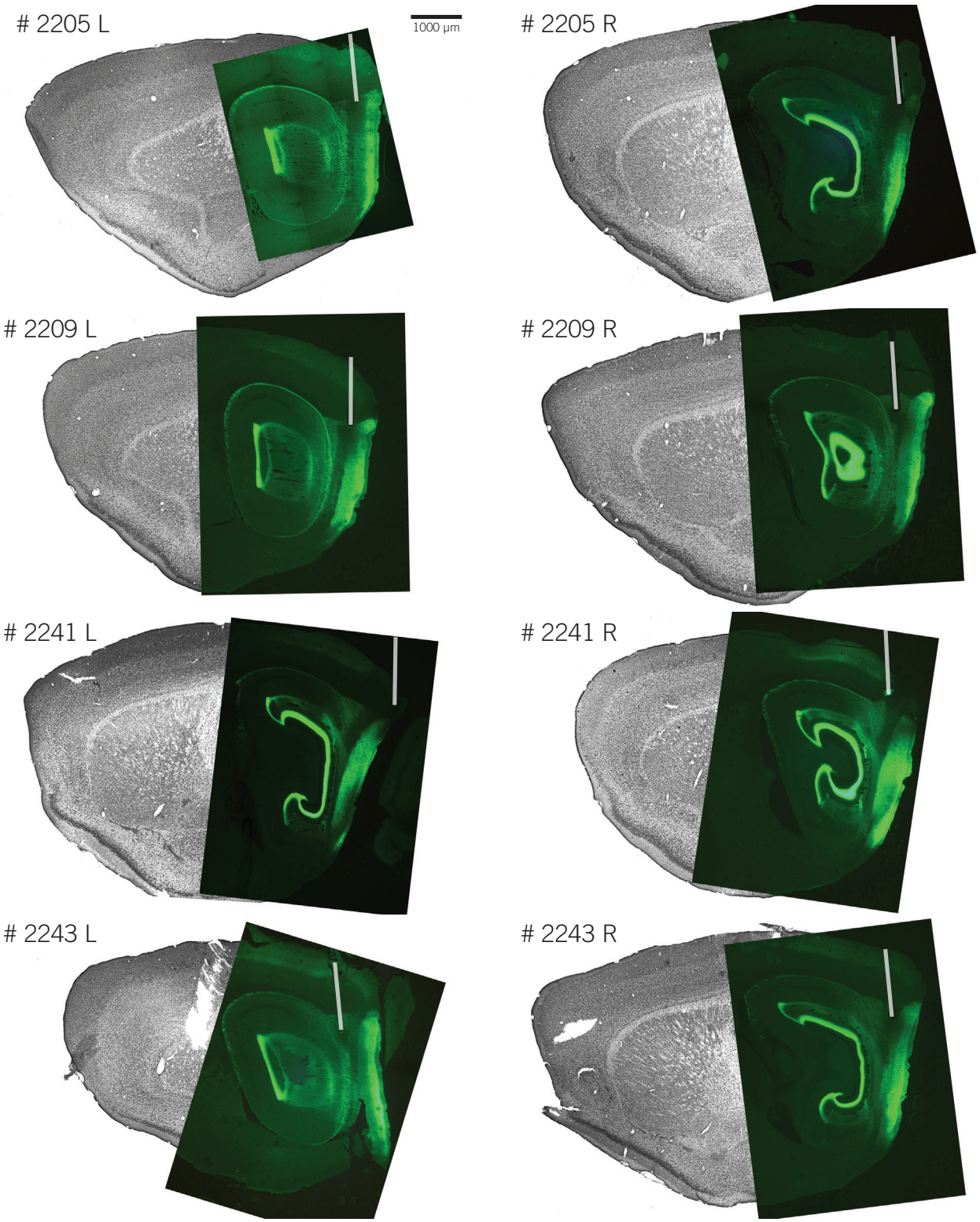

Sup. Figure 4 | **Experimental group (ENT x ARCH+/+) sagittal slices.** GFP expression. White line indicates fiber implant track.